Measurement and interpretation of differential cross sections for Higgs boson production at $\sqrt{s} = 13$ TeV

The CMS Collaboration *

CERN, Switzerland

ABSTRACT

Differential Higgs boson (H) production cross sections are sensitive probes for physics beyond the standard model. New physics may contribute in the gluon-gluon fusion loop, the dominant Higgs boson production mechanism at the LHC, and manifest itself through deviations from the distributions predicted by the standard model. Combined spectra for the H → $\gamma\gamma$, H → ZZ, and H → b$\overline{\text{b}}$ decay channels and the inclusive Higgs boson production cross section are presented, based on proton-proton collision data recorded with the CMS detector at $\sqrt{s} = 13$ TeV corresponding to an integrated luminosity of 35.9 fb^{-1}. The transverse momentum spectrum is used to place limits on the Higgs boson couplings to the top, bottom, and charm quarks, as well as its direct coupling to the gluon field. No significant deviations from the standard model are observed in any differential distribution. The measured total cross section is $61.1 \pm 6.0 \text{(stat)} \pm 3.7 \text{(syst)}$ pb, and the precision of the measurement of the differential cross section of the Higgs boson transverse momentum is improved by about 15% with respect to the H → $\gamma\gamma$ channel alone.

1. Introduction

The Higgs boson (H), whose existence is predicted by the Brout–Englert–Higgs mechanism [1–3], is responsible for electroweak symmetry breaking in the standard model (SM). Since the discovery [4–6] of a particle compatible with the SM Higgs boson at the CERN LHC, extensive effort has been dedicated to the measurement of its properties and couplings.

In this analysis we measure the inclusive and differential cross sections for the production of Higgs bosons. Compared with inclusive measurements [7–9], differential distributions provide extended information on the Higgs boson couplings, which can be extracted by fitting parametrized spectra to a combination of differential cross sections. When the Higgs boson couplings to quarks and to other bosons are varied with respect to their SM values, distortions of the predicted differential cross section spectra appear, which are particularly pronounced in the transverse momentum (p_T) distribution.

A precise measurement of the Higgs boson couplings represents an important test of the SM, as the couplings are sensitive to several SM extensions [10,11]. While the couplings to the top (y_t) and bottom (y_b) quarks are known with fair precision, there is

still a relatively large uncertainty in the measurement of the couplings to lighter quarks such as the coupling to the charm quark (y_c). A proof-of-concept study determining limits on the modification of the SM Higgs boson coupling (y_c^{SM}) to the charm quark, $\kappa_c = y_c/y_c^{\text{SM}}$, from the Higgs boson transverse momentum (p_T^H) distribution was performed in Ref. [12]. Reinterpreting the ATLAS Collaboration measurements in Ref. [13], this analysis yields the overall bounds $\kappa_c \in [-16, 18]$ at 95% confidence level (CL). Using the same data set, a reinterpretation of a search by the ATLAS Collaboration for the H → $J/\psi\gamma$ channel [14] yields $|\kappa_c| < 429$ at 95% CL [15]. More recently, studies from the ATLAS Collaboration [16, 17], using data collected at $\sqrt{s} = 13$ TeV corresponding to an integrated luminosity of 36.1 fb^{-1}, yield an observed upper limit on the H → J/ψ branching fraction of 3.5×10^{-4} at 95% CL that is an improvement of about a factor two with respect to the result obtained in Ref. [14], and an observed upper limit on the product of the production cross section and branching fraction $\sigma(\text{pp} \to \text{ZH})\mathcal{B}(\text{H} \to \text{c}\overline{\text{c}})$ of 110 times the SM value at 95% CL.

Both the ATLAS and CMS Collaborations have reported measurements of differential Higgs boson production cross sections at $\sqrt{s} = 8$ and 13 TeV [18–28]. The CMS Collaboration has measured differential Higgs boson production cross sections in the H → $\gamma\gamma$ [25] and H → ZZ$^{(*)}$ → 4ℓ ($\ell =$ e or μ) [27] decay channels using data recorded by the CMS experiment in 2016 at $\sqrt{s} = 13$ TeV, corresponding to an integrated luminosity of 35.9 fb^{-1}. We report

---

* *E-mail address:* cms-publication-committee-chair@cern.ch.

measurements of differential cross sections obtained by combining these results. Additionally, we include a search for the Higgs boson produced with large p_T and decaying to a bottom quark-antiquark ($b\bar{b}$) pair [29] in the combination of the p_T^H spectra. The differential cross sections for the following observables are combined: p_T^H, the Higgs boson rapidity $|y_H|$, the number of hadronic jets N_{jets}, and the transverse momentum of the leading hadronic jet p_T^{jet}.

We interpret the p_T^H spectrum in terms of Higgs boson couplings. In order to take into account as many degrees of freedom as possible, multiple couplings are varied simultaneously. We present results obtained by varying simultaneously (i) the modifier of the Higgs boson coupling to the charm quark κ_c and the bottom quark κ_b, (ii) the modifier of the Higgs boson coupling to the top quark κ_t and the coefficient c_g of the anomalous direct coupling to the gluon field in the heavy top quark mass limit, and (iii) κ_t and κ_b.

The SM production cross sections and decay rates depend on the Higgs boson mass m_H. We assume a Higgs boson mass of 125.09 GeV for all measurements in this paper, based on the combined ATLAS and CMS measurement using proton-proton collision data collected in 2011 and 2012 [8].

2. Theoretical predictions

Differential cross sections may be used to constrain model parameters. In the case of Higgs boson production via gluon fusion, the dominant production mode at the LHC, finite quark mass effects and moderate variations to Higgs boson couplings may manifest themselves through distortions of the p_T^H spectrum. We interpret the p_T^H spectrum for gluon fusion in terms of modifications of the couplings of the Higgs boson using two models: one tailored to heavy quarks and thus sensitive to effects at high p_T [30, 31], and the other considering the effect of lighter quarks in the gluon fusion loop [12]. The cross section for Higgs boson production in association with top quarks is taken to scale quadratically with κ_t. The other production processes are taken to be independent of these couplings. The coupling modifiers are described in the context of the κ-framework [32]:

$$\kappa_i = \frac{y_i}{y_i^{SM}}, \tag{1}$$

where y_i is the Higgs boson coupling to particle i. The SM value of any κ_i is equal to 1.

Recent developments in p_T resummation procedures have allowed more accurate calculations of the p_T^H spectrum when including the effects of lighter quarks on Higgs boson production via gluon fusion [33–36]. The p_T^H spectrum for gluon fusion has been calculated for simultaneous variations of κ_c and κ_b [12], taking into account the interference of the top quark loop with that from the bottom and charm quarks in the gluon fusion production loop, providing a novel approach to constrain these couplings via the p_T^H spectrum. We parameterize the variations computed in Ref. [12] with a quadratic polynomial for each bin of the p_T^H spectrum. The Higgs boson coupling to the top quark is fixed to its SM value in this model. The calculations from Ref. [12] are given up to the scale of the Higgs boson mass, and thus the $H \to b\bar{b}$ channel (for which the lower limit of the p_T^H spectrum is 350 GeV) is not used as input for the results obtained with this model.

A second model producing simultaneous variations of κ_t, c_g, and κ_b by adding dimension-6 operators to the SM Lagrangian has been built in Refs. [30,31]. This study employs an analytic resummation performed up to next-to-next-to-leading-logarithmic (NNLL) order in order to obtain the p_T^H spectrum at next-to-next-to-leading order+NNLL (NNLO+NNLL) accuracy. The dimension-6

operator whose coefficient is c_g yields a direct coupling of the Higgs field to the gluon field with the same underlying tensor structure as in the heavy-top mass limit. In the SM, the value of c_g equals 0. The introduction of c_g in the effective Lagrangian is given in Ref. [31] and the inclusive cross section is given by $\sigma \simeq \left|12c_g + \kappa_t\right|^2 \sigma^{SM}$. Two other operators are included in the Lagrangian to describe modifications of the top and bottom Yukawa couplings with coefficients κ_t and κ_b, respectively. While the model allows simultaneous variation of all three coupling modifiers, we consider only simultaneous variations of κ_t and c_g, and of κ_t and κ_b. The precomputed spectra from Ref. [30] are used as input and parametrized using a quadratic polynomial.

3. The CMS detector

The central feature of the CMS apparatus is a superconducting solenoid of 6 m internal diameter, providing a magnetic field of 3.8 T. Within the solenoid volume are a silicon pixel and strip tracker, a lead tungstate crystal electromagnetic calorimeter, and a brass and scintillator hadron calorimeter, each composed of a barrel and two endcap sections. Forward calorimeters extend the pseudorapidity (η) coverage provided by the barrel and endcap detectors. Muons are detected in gas-ionization chambers embedded in the steel flux-return yoke outside the solenoid. A more detailed description of the CMS detector, together with a definition of the coordinate system used and the relevant kinematic variables, can be found in Ref. [37].

4. Inputs to the combined analysis

For all the analyses used as input to the combination (H $\to$ $\gamma\gamma$ [25], H $\to$ ZZ$^{(*)} \to 4\ell$ [27], and H $\to$ b$\bar{b}$ [29]), the data set corresponds to an integrated luminosity of 35.9 fb^{-1} recorded by the CMS experiment in 2016. The H $\to$ b$\bar{b}$ decay channel is only included in the combination of the p_T^H spectra, improving the measurements at the higher end of the distribution where the data from the H $\to$ $\gamma\gamma$ and H $\to$ ZZ decay channels are limited. All analyses provide the parametrization of the folding matrix M_{ji}^k (which is the probability for an event in generator-level bin i to be reconstructed in bin j and category k) in terms of a common generator-level binning, that is used for the combined spectra. Given the limited statistical precision in the individual channels, the results of the H $\to$ ZZ and H $\to$ b$\bar{b}$ channels individually are reported for a coarser binning, which is provided in Tables 1–4 for each of the observables. This binning coincides with the binning at the reconstruction level.

The SM prediction for the differential cross sections is simulated with MADGRAPH5_aMC@NLO v2.2.2 [38] for each of the four dominant Higgs boson production modes: gluon-gluon fusion (ggH), vector boson fusion, associated production with a W/Z boson, and associated production with a top quark-antiquark pair. A contribution from Higgs boson production in association with bottom quarks is not simulated, but included assuming its acceptance is equal to that from Higgs boson production via gluon fusion. The matrix element calculation includes the emission of up to two additional partons and is performed at NLO accuracy in perturbative quantum chromodynamics (QCD). Events are interfaced to PYTHIA 8.205 [39] for parton showering and hadronization with the CUETP8M1 [40] underlying event tune. The matrix element calculation is matched to the parton shower following the prescription in Ref. [41]. A weight depending on p_T^H and N_{jets} is applied to simulated ggH events to match the predictions from the NNLOPS program [42,43], as discussed in Ref. [9]. The set of parton distribution functions used in all simulations is NNPDF3.0 [44]. The hadronic jets are clustered from the particle-flow candidates [45]

Table 1

The reconstruction-level binning for p_T^H for the H $\to \gamma\gamma$, H $\to$ ZZ, and H $\to$ b$\bar{\text{b}}$ channels. This binning coincides with the binning of the unfolded cross sections in which the individual results are reported.

Channel	p_T^H binning (GeV)								
H $\to \gamma\gamma$	[0, 15)	[15, 30)	[30, 45)	[45, 80)	[80, 120)	[120, 200)	[200, 350)	[350, 600)	[600, ∞)
H $\to$ ZZ	[0, 15)	[15, 30)	[30, 80)		[80, 200)		[200, ∞)		
H $\to$ b$\bar{\text{b}}$	None							[350, 600)	[600, ∞)

in the case of data and simulation, and from stable particles excluding neutrinos in the case of generated events, using the anti-k_T clustering algorithm [46] with a distance parameter of 0.4. The measurements are reported in terms of kinematic observables defined before the decay of the Higgs boson, i.e. at the generator level.

Each of the analyses used as input to the combination corresponds to a different fiducial phase space definition and applies a different event categorization. In the case of the H $\to \gamma\gamma$ analysis, the fiducial phase space is defined by requiring the ratio of the leading (subleading) photon p_T to the diphoton mass to be greater than 1/3 (1/4). In addition, for each photon candidate the scalar sum of the generator-level p_T of stable particles contained in a cone of radius $\Delta R = 0.3$ around the candidate is required to be less than 10 GeV, where $\Delta R = \sqrt{(\Delta\eta)^2 + (\Delta\phi)^2}$ is the angular separation between particles and $\Delta\phi$ is the azimuthal angle between two particles in radians. The selected photon pairs are categorized according to their estimated relative invariant mass resolution [25]. In the case of the H $\to$ ZZ analysis, the 4-lepton mass is required to be greater than 70 GeV, the leading Z boson candidate invariant mass must be greater than 40 GeV, and leptons must be separated in angular space by at least $\Delta R > 0.02$. Furthermore, at least two leptons must each have a $p_T > 10$ GeV and at least one a $p_T > 20$ GeV. The selected events are categorized according to their lepton configuration in the final state (4 electrons, 4 muons, or 2 electrons and 2 muons). In the case of the H $\to$ b$\bar{\text{b}}$ analysis, the analysis strategy requires the presence of a single anti-k_T jet with a distance parameter of 0.8, $p_T > 450$ GeV, and $|\eta| < 2.5$. For this analysis, the data is not unfolded to a fiducial phase space. Soft and wide-angle radiation is removed using the soft-drop grooming algorithm [47,48]. The jet mass after application of the soft-drop algorithm, m_{SD}, peaks close to the Higgs boson mass in the case of signal events. To avoid finite-cone effects and the nonperturbative regime of the m_{SD} calculation, events are selected based on the dimensionless mass scale variable for QCD jets defined as $\rho = \log\left(m_{SD}^2/p_T^2\right)$ [47], which relates the jet p_T to the jet mass. Events with isolated electrons, muons, or τ leptons with $p_T > 10$ GeV and $|\eta| < 2.5$ are vetoed in order to reduce the background from SM electroweak processes, and events with a missing transverse momentum greater than 140 GeV are vetoed in order to reduce the background from top quark-antiquark pair production. Additionally, a selection criterion is applied based on the compatibility of the single anti-k_T jet with having a two-prong substructure [49–52]. Events are categorized according to their likelihood of consisting of two b quarks, which is computed using the double-b tagger algorithm [53].

Minor modifications are applied to the individual analyses in Refs. [25,27,29] to provide the inputs used for the combination of differential observables. For H $\to \gamma\gamma$, an additional bin, $p_T^H > 600$ GeV, is included in the p_T^H spectrum. For H $\to$ ZZ, the binning is modified for multiple kinematic observables to align with the binning of the H $\to \gamma\gamma$ analysis. Furthermore, the branching fractions of the two Z bosons to the various lepton configurations are fixed to their SM values, whereas in Ref. [27] these are allowed to float. For H $\to$ b$\bar{\text{b}}$ the signal is split into two p_T bins at the generator level: the first with $350 \le p_T < 600$ GeV, where the lower

Table 2

The binning for N_{jets} for the H $\to \gamma\gamma$ and the H $\to$ ZZ channels. This binning coincides with the binning of the unfolded cross sections in which the individual results are reported.

Channel	N_{jets} binning				
H $\to \gamma\gamma$	0	1	2	3	≥ 4
H $\to$ ZZ	0	1	2	≥ 3	

limit has been extended downwards with respect to the individual analysis, and the second an overflow bin with $p_T \ge 600$ GeV, which aligns with the binning of the other channels. At the reconstruction level two bins are employed, with $450 \le p_T < 600$ and $p_T \ge 600$ GeV, which is a slight modification with respect to the binning used in Ref. [29]. The redefinition of the reconstructed p_T categories necessitates a reevaluation of the background model, which is performed using the same procedure as in the original analysis. For the purpose of the combination in this analysis, the fiducial measurements from the H $\to \gamma\gamma$ and H $\to$ ZZ channels are extrapolated to the inclusive phase space [38,42,43].

5. Statistical analysis

The cross sections are extracted through a simultaneous extended maximum likelihood fit to the diphoton mass, four-lepton mass, and m_{SD} distributions in all the analysis categories of the H $\to \gamma\gamma$, H $\to$ ZZ, and H $\to$ b$\bar{\text{b}}$ channels, respectively.

The number of expected signal events n^{sig} in a given reconstructed kinematic bin i, given analysis category k and given decay channel m is obtained from:

$$n_i^{\text{sig}, km}(\vec{\Delta\sigma}|\vec{\theta}) = \sum_{j=1}^{n_{\text{bins}}^{\text{gen}}} \Delta\sigma_j \, L(\vec{\theta}) \, \mathcal{B}^m \, M_{ji}^{km}(\vec{\theta}), \qquad (2)$$

where:

- j is a kinematic bin index at the generator level;
- $n_{\text{bins}}^{\text{gen}}$ is the number of kinematic bins at the generator level, which is the same for all decay channels;
- $\vec{\Delta\sigma}$ is the set of differential cross sections at the generator level, and L is the integrated luminosity of the samples used in this analysis;
- $\mathcal{B}^m$ is the branching fraction of the decay channel m. The overall effect of the branching fraction uncertainties on the combined spectra is below 1%, and has been neglected.
- M_{ji}^{km} is the folding matrix, which is determined from Monte Carlo simulation; note that the corresponding matrix $\vec{M}^{km}$ need not be square; the number of reconstructed bins may be smaller than the number of bins at the generator level; and
- $\vec{\theta}$ is the set of nuisance parameters.

The bin-to-bin migrations are taken into account via the folding matrix, effectively allowing unfolding of the detector effects. Following the prescription in Ref. [54], we find that no regularization of the unfolding procedure is needed.

An extended likelihood function for a single decay channel m is constructed:

Table 3

The binning for $|y_H|$ for the H $\to \gamma\gamma$ and the H $\to$ ZZ channels. This binning coincides with the binning of the unfolded cross sections in which the individual results are reported.

Channel	$|y_H|$ binning					
H $\to \gamma\gamma$	[0.0, 0.15)	[0.15, 0.30)	[0.30, 0.60)	[0.60, 0.90)	[0.90, 1.20)	[1.20, 2.50]
H $\to$ ZZ	[0.0, 0.15)	[0.15, 0.30)	[0.30, 0.60)	[0.60, 0.90)	[0.90, 1.20)	[1.20, 2.50]

Table 4

The binning for p_T^{jet} for the H $\to \gamma\gamma$ and the H $\to$ ZZ channels. This binning coincides with the binning of the unfolded cross sections in which the individual results are reported.

Channel	p_T^{jet} binning (GeV)					
H $\to \gamma\gamma$	[0, 30)	[30, 55)	[55, 95)	[95, 120)	[120, 200)	[200, ∞)
H $\to$ ZZ	[0, 30)	[30, 55)	[55, 95)	[95, ∞)		

$$\mathcal{L}_m(\vec{\Delta\sigma}|\vec{\theta}) = \prod_{i=1}^{n_{\text{bins}}^{\text{reco}, m}} \prod_{k=1}^{n_{\text{cat}}^{m}} \prod_{l=1}^{n_{\mathcal{O}}^{m}} \left(\text{pdf}_i^{km}(\mathcal{O}_l^m|\vec{\Delta\sigma}, \vec{\theta}) \right)^{N_{\text{obs}}^{iklm}}$$

$$\times \text{Poisson}\left(N_{\text{obs}}^{ikm} \left| n_i^{\text{sig}, km}(\vec{\Delta\sigma}|\vec{\theta}) + n_i^{\text{bkg}, km}(\vec{\theta}) \right. \right), \quad (3)$$

where:

- $\mathcal{O}^m$ is the observable, i.e. the diphoton mass, the four-lepton mass, or m_{SD} for the H $\to \gamma\gamma$, H $\to$ ZZ, and H $\to$ b$\bar{\text{b}}$ decay channels, respectively;
- $n_{\text{bins}}^{\text{reco}, m}$ is the number of reconstructed bins, n_{cat}^m is the number of categories for the decay channel (see the individual analyses [25,27,29] for more details), and $n_{\mathcal{O}}^m$ is the number of bins for observable $\mathcal{O}$;
- N_{obs}^{iklm} is the number of observed events reconstructed in kinematic bin i, category k and observable bin l, and N_{obs}^{ikm} is the same but summed over all bins of the observable;
- $n_i^{\text{bkg}, km}$ is the number of expected background events; and
- $\text{pdf}_i^{km}(\mathcal{O}_l^m|\vec{\Delta\sigma}, \vec{\theta})$ is the probability density function for the observable, based on the signal and background distributions of the observable which are determined via simulation.

In order to combine the decay channels, the likelihoods for the individual decay channels are multiplied:

$$\mathcal{L}(\vec{\Delta\sigma}|\vec{\theta}) = \prod_{m=1}^{n_c} \mathcal{L}_m(\vec{\Delta\sigma}|\vec{\theta}) \, \text{pdf}(\vec{\theta}), \quad (4)$$

where n_c is the number of decay channels included in the combination, $\mathcal{L}_m$ is the likelihood formula from Eq. (3) specific to the decay channel m, and $\text{pdf}(\vec{\theta})$ is the probability density function of the nuisance parameters. For the individual analyses, the number of categories, invariant mass bins, and even the number of reconstructed bins may differ, although the number of bins at the generator level and their binning need to be aligned between decay channels. Note that a single common set of differential cross sections and nuisance parameters is fitted to the data in all decay channels simultaneously.

The test statistic q, which is asymptotically distributed as a χ^2, is defined as [55,56]:

$$q(\vec{\Delta\sigma}) = -2 \ln \left(\frac{\mathcal{L}\left(\vec{\Delta\sigma} \left| \hat{\hat{\vec{\theta}}}_{\vec{\Delta\sigma}} \right.\right)}{\mathcal{L}\left(\hat{\vec{\Delta\sigma}} \left| \hat{\vec{\theta}} \right.\right)} \right). \quad (5)$$

The quantities $\hat{\vec{\Delta\sigma}}$ and $\hat{\vec{\theta}}$ are the unconditional maximum likelihood estimates for the parameters $\vec{\Delta\sigma}$ and $\vec{\theta}$, respectively, while $\hat{\hat{\vec{\theta}}}_{\vec{\Delta\sigma}}$ denotes the maximum likelihood estimate for $\vec{\theta}$ conditional on the values of $\vec{\Delta\sigma}$.

The Higgs boson coupling modifiers are fitted via a largely analogous procedure. In the likelihood function (4), the differential cross sections $\vec{\Delta\sigma}$ are replaced by parametrizations of theoretical spectra, instead of allowing them to be determined in the fit:

$$\vec{\Delta\sigma} \to \vec{\Delta\sigma}(\kappa_a, \kappa_b), \quad (6)$$

where κ_a and κ_b are the coupling modifiers to be fitted.

6. Systematic uncertainties

The experimental systematic uncertainties from the input analyses are incorporated in the combination as nuisance parameters in the extended likelihood fit and are profiled. Among the decay channels, correlations are taken into account for the systematic uncertainties in the jet energy scale and resolution, and the integrated luminosity. Detailed descriptions of the experimental systematic uncertainties per decay channel can be found in Refs. [25, 27,29].

The measurement is made for the full phase space rather than limited to a fiducial phase space (as is the case for the original H $\to \gamma\gamma$ and H $\to$ ZZ analyses). This means that the uncertainties in the acceptances for the individual analyses and in the branching fractions may affect the results. The effect of the acceptance uncertainties per bin on the overall uncertainty, including the effect of the Higgs coupling modifiers on the acceptances, is less than 1% and so this is neglected in the combination. For certain measurements the production cross sections of non-ggH production modes are assumed to be their respective SM value. In these cases, the uncertainty in the inclusive production cross section from non-ggH modes, determined to be about 2.1% [57], has been taken into account as a nuisance parameter.

The theoretical predictions described in Section 2 are subject to theoretical uncertainties from the renormalisation scale μ_R and the factorisation scale μ_F. The standard approach to evaluate the impact of these uncertainties is to compute an envelope of scale variations, and to assign the extrema of the envelope as the uncertainty. To this end, μ_R and μ_F are independently varied between 0.5, 1, and 2 times their nominal value, whereas the fraction $\frac{\mu_R}{\mu_F}$ is constrained not to be less than 0.5 or greater than 2.0. As the theoretical spectra in the $\kappa_t/c_g/\kappa_b$ case and the κ_c/κ_b case contain a resummation, the uncertainty in the resummation scale Q is also considered, and it is evaluated by varying Q from 0.5 to 2 times its central value (while keeping μ_F and μ_R at their respective central values). The theoretical uncertainties are assigned by applying the minimum and maximum scale variations per bin. The resulting uncertainties for the spectra under variations of κ_b and κ_c and variations of κ_t, c_g, and κ_b are shown in Tables 5 and 6, respectively.

Table 5
Uncertainties in the predicted p_T^H spectra related to variations of theory parameters for the κ_b and κ_c case.

Binning (GeV)	[0, 15)	[15, 30)	[30, 45)	[45, 80)	[80, 120)
Δ^{scale} (%)	8.9%	6.6%	18.1%	22.0%	21.6%

Table 6
Uncertainties in the predicted p_T^H spectra related to variations of theory parameters for the κ_t, c_g, and κ_b case.

Binning (GeV)	[0, 15)	[15, 30)	[30, 45)	[45, 80)	[80, 120)	[120, 200)	[200, 350)	[350, 600)	[600, 800)
Δ^{scale} (%)	12.7%	7.4%	9.5%	12.8%	17.4%	19.3%	20.9%	23.4%	8.2%

Theoretical uncertainties are subject to bin-to-bin correlations. We adopt a procedure that produces a correlation coefficient ρ_{ab} directly from the individual scale variations:

$$\rho_{ab} = \frac{\sum_i (\sigma_{a,i} - \overline{\sigma}_a)(\sigma_{b,i} - \overline{\sigma}_b)}{\sqrt{\sum_i (\sigma_{a,i} - \overline{\sigma}_a)^2 \sum_i (\sigma_{b,i} - \overline{\sigma}_b)^2}}, \quad (7)$$

where $\sigma_{a(b),i}$ is the cross section in bin a (b) of the ith scale variation, $\overline{\sigma}_{a(b)}$ is the mean cross section in bin a (b), and ρ_{ab} is the resulting correlation coefficient between bin a and b. The correlation structure is characterized by strong correlations among bins at moderate p_T^H ($15 \le p_T^H \le 600$ GeV). Only the bins with $p_T^H < 15$ and $p_T^H > 600$ GeV are anti-correlated with the bins at moderate p_T^H.

7. Results

7.1. Total cross section and $\mathcal{B}_{\gamma\gamma}/\mathcal{B}_{ZZ}$

The total cross section for Higgs boson production, based on a combination of the $H \to \gamma\gamma$ and $H \to ZZ$ channels, is measured to be $61.1 \pm 6.0\,(\text{stat}) \pm 3.7\,(\text{syst})$ pb, obtained by applying the treatment described in Section 4 to the inclusive cross section (i.e. with a single bin, both at generator and at reconstruction level). The measured total cross sections from the individual channels are 64.0 ± 9.6 pb for $H \to \gamma\gamma$ and 58.2 ± 9.8 pb for $H \to ZZ$; the combination improves the precision by 27% with respect to the $H \to \gamma\gamma$ channel individually. The likelihood scans for the individual decay channels and their combination are shown in Fig. 1 (upper). The combination result agrees with the SM value of 55.6 ± 2.5 pb [57].

A measurement of the branching fraction for one decay channel is degenerate with a measurement of the total cross section. However, the ratio of branching fractions for two decay channels can be measured while profiling the total cross section. The ratio of the $H \to \gamma\gamma$ and $H \to ZZ$ branching fractions, $\mathcal{B}_{\gamma\gamma}/\mathcal{B}_{ZZ}$, is measured to be $0.092 \pm 0.018\,(\text{stat}) \pm 0.010\,(\text{syst})$. This is in agreement with the SM prediction of 0.086 ± 0.002 [57]. The likelihood scan for $\mathcal{B}_{\gamma\gamma}/\mathcal{B}_{ZZ}$ is shown in Fig. 1 (lower).

7.2. Combinations of differential observables

The unfolded differential cross sections for the observables p_T^H, N_{jets}, $|y_H|$, and p_T^{jet} are shown in Figs. 2, 3, 4, and 5, respectively. Fig. 2 (lower) shows the differential cross section of p_T^H for Higgs boson production via gluon fusion; for this result, the non-gluon-fusion production modes are considered to be background, constrained to the SM predictions with their respective uncertainties. The numerical values for the spectra in Figs. 2–5 are given in Appendix A and the corresponding bin-to-bin correlation matrices are given in Appendix B. For the observables p_T^H, N_{jets}, and p_T^{jet}, the rightmost bin is an overflow bin, which is normalized by the bin width of the second-to-rightmost bin. Overall no significant deviations from the SM predictions are observed. For the p_T^H
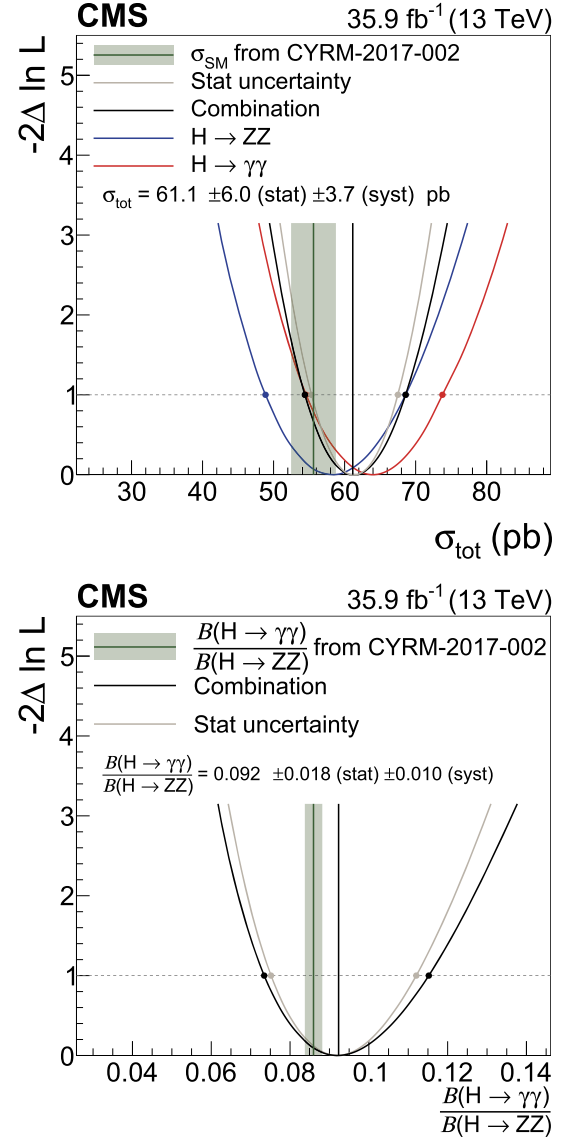

Fig. 1. Scan of the total cross section σ_{tot} (upper) and of the ratio of branching fractions $\mathcal{B}_{\gamma\gamma}/\mathcal{B}_{ZZ}$ (lower), based on a combination of the $H \to \gamma\gamma$ and $H \to ZZ$ analyses. The markers indicate the one standard deviation confidence interval. *CYRM-2017-002* refers to Ref. [57].

spectrum, the dominant source of uncertainty is the statistical one; in particular, the systematic uncertainty is about half the statistical uncertainty in the rightmost bin, and much smaller than the statistical uncertainty in all other bins. The total uncertainty in the combination per bin varies between 30 and 40%. Compared to the measurement in the $H \to \gamma\gamma$ channel alone, the decrease in uncer-
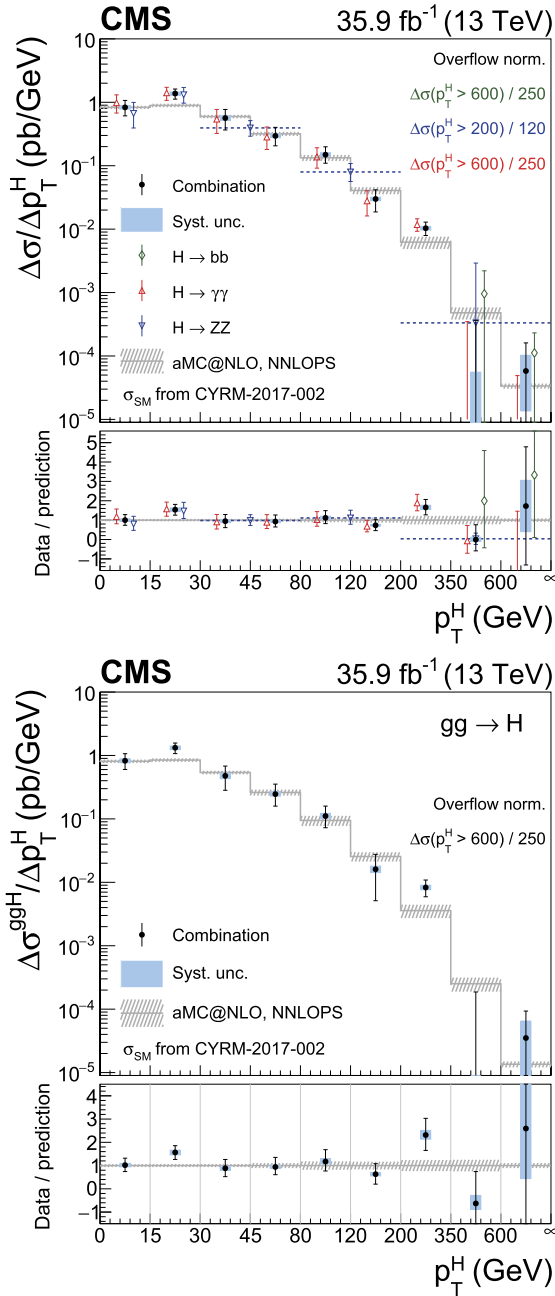
Fig. 2. Measurement of the total differential cross section (upper) and the differential cross section of gluon fusion (lower) as a function of p_T^H. The combined spectrum is shown as black points with error bars indicating a 1 standard deviation uncertainty. The systematic component of the uncertainty is shown by a blue band. The spectra for the $H \to \gamma\gamma$, $H \to ZZ$, and $H \to b\bar{b}$ channels are shown in red, blue, and green, respectively. The dotted horizontal lines in the $H \to ZZ$ channel indicate the coarser binning of this measurement. The rightmost bins of the distributions are overflow bins; the normalizations of the cross sections in these bins are indicated in the figure. *CYRM-2017-002* refers to Ref. [57].

tainty achieved by the combination is most notable in the low-p_T region. The contribution of the $H \to b\bar{b}$ channel to the overall precision of the combination is most significant in the last p_T^H bin.

7.3. Fits of Higgs boson coupling modifiers: κ_b vs. κ_c

Fig. 6 (upper) shows the one and two standard deviation contours of the fits of the κ_b/κ_c parametrization from Ref. [12] to data, assuming the branching fractions are dependent on the Higgs
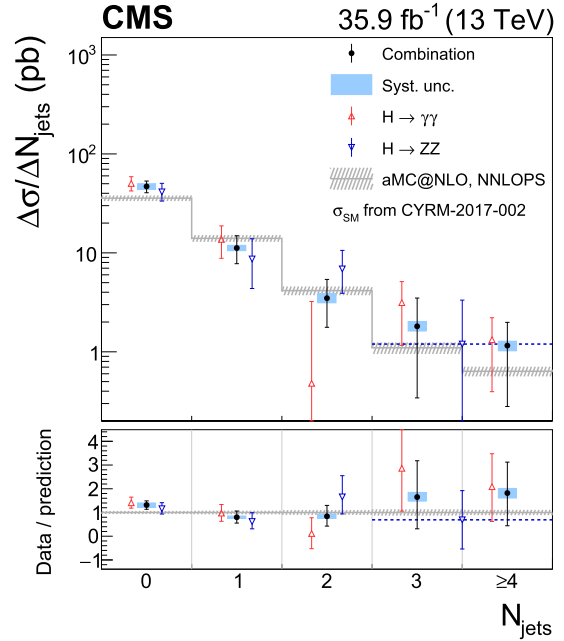
Fig. 3. Measurement of the differential cross section as a function of N_{jets}. The combined spectrum is shown as black points with error bars indicating a 1 standard deviation uncertainty. The systematic component of the uncertainty is shown by a blue band. The spectra for the $H \to \gamma\gamma$ and $H \to ZZ$ channels are shown in red and blue, respectively. The dotted horizontal lines in the $H \to ZZ$ channel indicate the coarser binning of this measurement. *CYRM-2017-002* refers to Ref. [57].
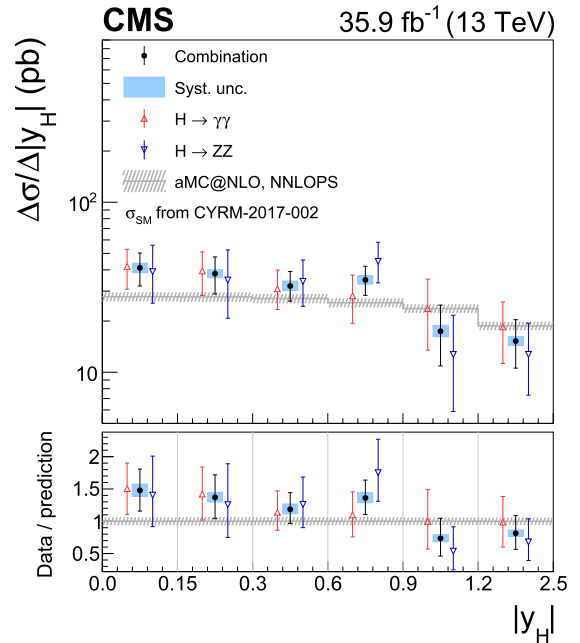

Fig. 4. Measurement of the differential cross section as a function of $|y_H|$. The combined spectrum is shown as black points with error bars indicating a 1 standard deviation uncertainty. The systematic component of the uncertainty is shown by a blue band. The spectra for the $H \to \gamma\gamma$ and $H \to ZZ$ channels are shown in red and blue, respectively. *CYRM-2017-002* refers to Ref. [57].

boson couplings, i.e., $\mathcal{B} = \mathcal{B}(\kappa_b, \kappa_c)$, and that there are no beyond-the-SM contributions. The substructure on the combined scan shows a ring shape around the origin, in agreement with the SM prediction within one standard deviation.
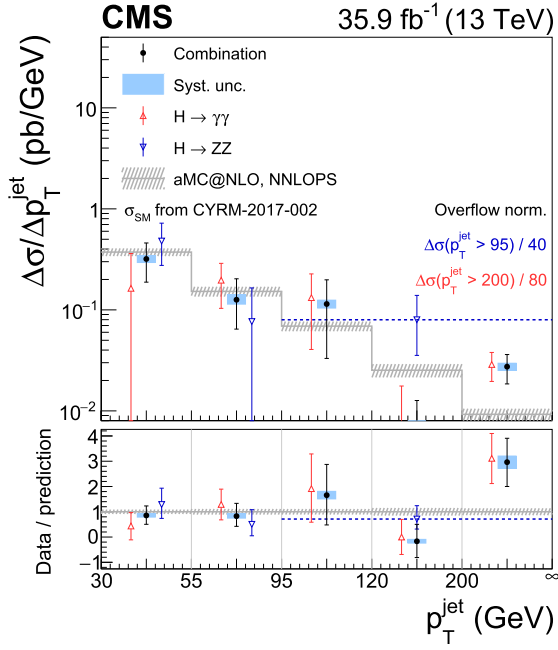
Fig. 5. Measurement of the differential cross section as a function of p_T^{jet}. The combined spectrum is shown as black points with error bars indicating a 1 standard deviation uncertainty. The systematic component of the uncertainty is shown by a blue band. The spectra for the $H \to \gamma\gamma$ and $H \to ZZ$ channels are shown in red and blue, respectively. The dotted horizontal lines in the $H \to ZZ$ channel indicate the coarser binning of this measurement. The rightmost bin of the distribution is an overflow bin; the normalization of the cross section in that bin is indicated in the figure. *CYRM-2017-002* refers to Ref. [57].

In order to assess the constraint obtained only from the knowledge of the p_T^H distribution, the total width and the overall normalization are profiled in the fit. This is effectively accomplished by implementing the branching fractions for the $H \to \gamma\gamma$ and $H \to ZZ$ channels as nuisance parameters with no prior constraint, i.e. as free parameters. The result of this fit is shown in Fig. 6 (lower). As expected, the range of allowed values of κ_b and κ_c is much wider than in the case of coupling-dependent branching fractions.

Confidence intervals can be set on κ_b and κ_c by profiling one coupling and scanning over the other. The results of these single-coupling scans are shown in Figs. 7 and 8. The observed (expected) limits at 95% CL in the one-dimensional scans are:

$$-1.1 < \kappa_b < 1.1(-1.3 < \kappa_b < 1.3),$$
$$-4.9 < \kappa_c < 4.8(-6.1 < \kappa_c < 6.0), \tag{8}$$

in the case of branching fractions that depend on κ_b and κ_c, and

$$-8.5 < \kappa_b < 18(-8.8 < \kappa_b < 15),$$
$$-33 < \kappa_c < 38 \ (-31 < \kappa_c < 36), \tag{9}$$

in the case of the branching fractions implemented as nuisance parameters with no prior constraint. For the coupling-dependent branching fractions, the results are shaped predominantly by the constraints from the total width rather than by distortions of the p_T^H spectrum. If the branching fractions are fixed to their SM expectations, the one-dimensional scans yield the following expected limits at 95% CL:

$$-3.5 < \kappa_b < 5.1,$$
$$-13 < \kappa_c < 15. \tag{10}$$

These intervals are comparable to those in Ref. [12], where $\kappa_c \in [-16, 18]$ at 95% CL, noting that the results here are based on a
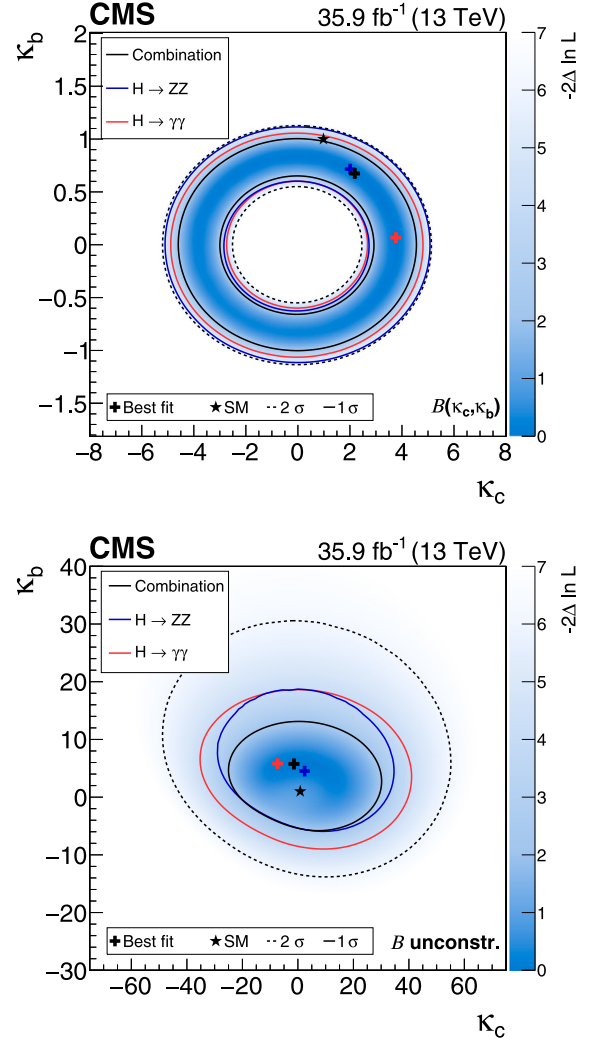
larger data set. The intervals obtained are competitive with the intervals from other direct search channels summarized in Section 1.

7.4. Fits of Higgs boson coupling modifiers: κ_t vs. c_g and κ_t vs. κ_b

The fits are repeated in a way analogous to that of Section 7.3 but with κ_t, c_g, and κ_b, the coefficients of the dimension-6 operators added to the SM Lagrangian, as the parameters of the fit, using the parametrization obtained from Refs. [30,31]. The combined log-likelihood scan for κ_t vs. c_g, assuming branching fractions that depend on the couplings, is shown in Fig. 9 (upper). The normalization of the spectrum is, by construction, equal to the SM normalization for the set of coefficients satisfying $12c_g + \kappa_t \simeq 1$. The shape of the parametrized p_T^H spectrum s is calculated by normalizing the differential cross section to 1:

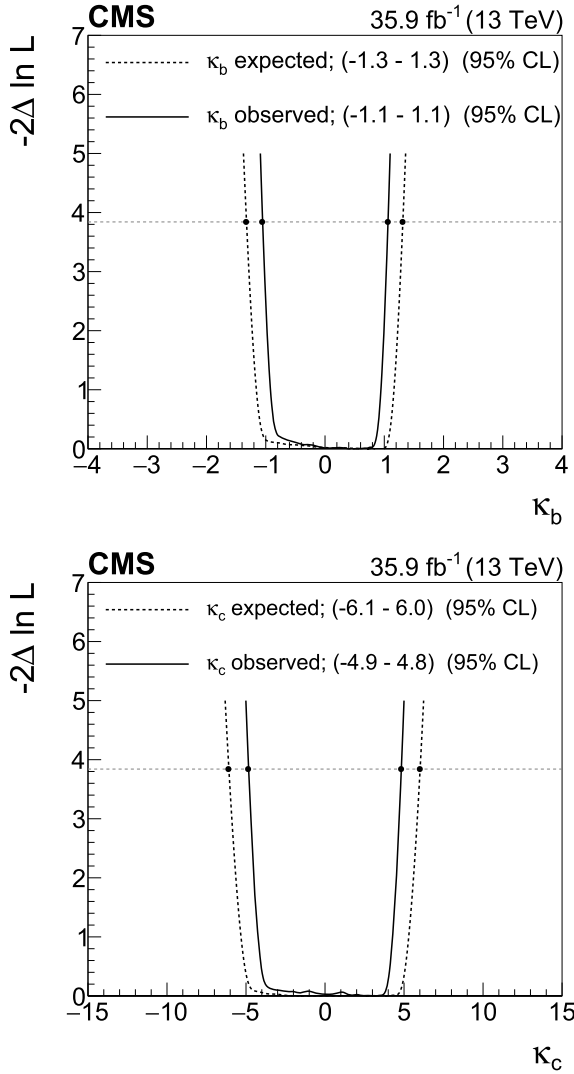$$s_i(\kappa_t, c_g) = \frac{\sigma_i(\kappa_t, c_g)}{\sum_j \sigma_j(\kappa_t, c_g)}, \tag{11}$$

Fig. 6. Simultaneous fit to data for κ_b and κ_c, assuming a coupling dependence of the branching fractions (upper) and the branching fractions implemented as nuisance parameters with no prior constraint (lower). The one standard deviation contour is drawn for the combination ($H \to \gamma\gamma$ and $H \to ZZ$), the $H \to \gamma\gamma$ channel, and the $H \to ZZ$ channel in black, red, and blue, respectively. For the combination the two standard deviation contour is drawn as a black dashed line, and the shading indicates the negative log-likelihood, with the scale shown on the right hand side of the plots.

Fig. 7. Likelihood scan of κ_b while profiling κ_c (upper), and of κ_c while profiling κ_b (lower). The filled markers indicate the limits at 95% CL. The branching fractions are considered dependent on the values of the couplings.

Fig. 8. Likelihood scan of κ_b while profiling κ_c (upper), and of κ_c while profiling κ_b (lower). The filled markers indicate the limits at 95% CL. The branching fractions are implemented as nuisance parameters with no prior constraint.

where σ_i is the parametrization in bin i. Inserting the expected parabolic dependence of $\sigma_i(\kappa_t, c_g)$ reveals that the shape of the parametrization for κ_t/c_g variations becomes a function of the ratio of the two couplings, $s_i(c_g/\kappa_t)$. Thus the dependence of the likelihood on the radial distance $\sqrt{\kappa_t^2 + c_g^2}$ stems from constraints on the overall normalization, whereas the dependence on the slope c_g/κ_t stems from constraints on the shape of the distribution. The dependence of the likelihood on the slope becomes apparent in Fig. 9 (lower), where the branching fractions are implemented as nuisance parameters with no prior constraint in the fit. Except at small values of the couplings, the constraint on the couplings comes from their ratio. The two symmetric sets of contours are due to a symmetry of the parametrization under $(\kappa_t, c_g) \to (-\kappa_t, -c_g)$. The constraint from the H $\to \gamma\gamma$ channel individually is here slightly stronger than the combination; this effect, not observed in expected fits, stems from opposite deviations in the H $\to \gamma\gamma$ and H $\to$ ZZ p_T^H spectra that cancel out in the combination.

Fig. 10 (upper) shows the combined log-likelihood scan as a function of κ_t and κ_b, with branching fractions scaling appropriately with the coupling modifiers and Fig. 10 (lower) with the branching fractions implemented as nuisance parameters with no
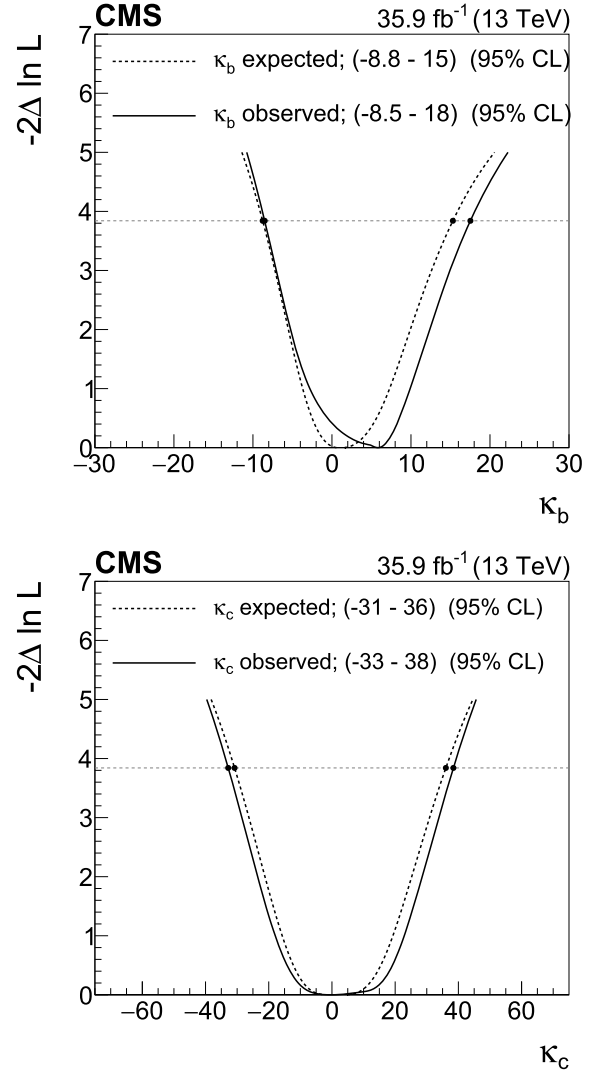
prior constraint. As the H $\to \gamma\gamma$ branching fraction depends linearly on κ_t, the constraints on the H $\to \gamma\gamma$ channel and the combination in Fig. 10 (upper) are not symmetric with respect to the κ_t axis. For the branching fractions implemented as nuisance parameters with no prior constraint, the parametrization is symmetric under $(\kappa_t, \kappa_b) \to (-\kappa_t, -\kappa_b)$, which explains the observed symmetry in Fig. 10 (lower).

8. Summary

A combination of differential cross sections for the Higgs boson transverse momentum p_T^H, the number of jets, the rapidity of the Higgs boson, and the p_T of the leading jet has been presented, using proton-proton collision data collected at $\sqrt{s} = 13$ TeV with the CMS detector, corresponding to an integrated luminosity of 35.9 fb^{-1}. The spectra obtained are based on data from the H $\to \gamma\gamma$, H $\to$ ZZ, and H $\to$ b$\bar{\text{b}}$ decay channels. The precision of the combined measurement of the differential cross section of p_T^H is improved by about 15% with respect to the H $\to \gamma\gamma$ channel alone. The improvement is larger in the low-p_T^H region than in the high-p_T^H tails. No significant deviations from the standard model are observed in any differential distribution. Additionally,
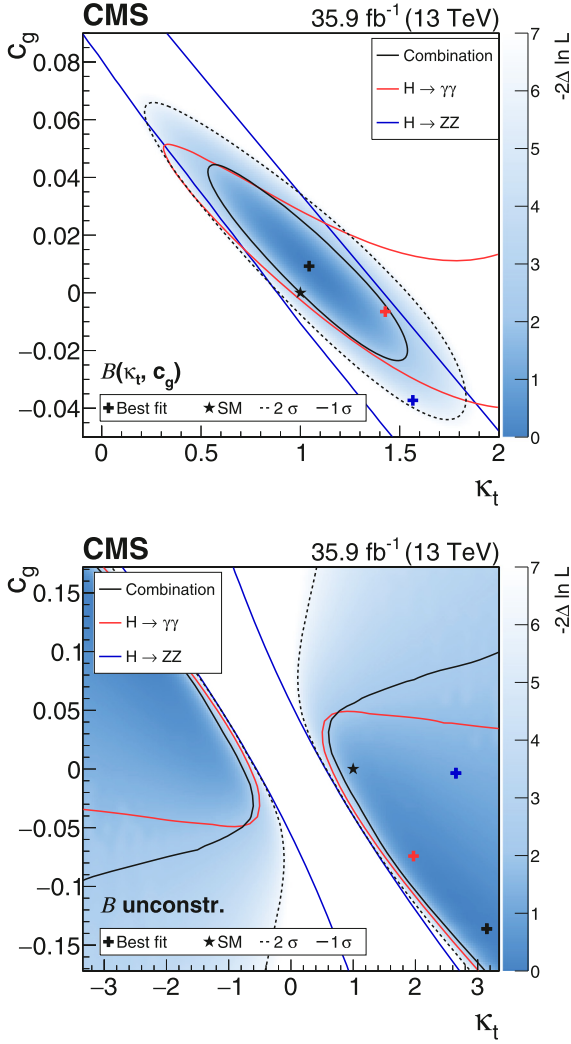
Fig. 9. Simultaneous fit to data for κ_t and c_g, assuming a coupling dependence of the branching fractions (upper) and the branching fractions implemented as nuisance parameters with no prior constraint (lower). The one standard deviation contour is drawn for the combination ($H \to \gamma\gamma$, $H \to ZZ$, and $H \to b\bar{b}$), the $H \to \gamma\gamma$ channel, and the $H \to ZZ$ channel in black, red, and blue, respectively. For the combination the two standard deviation contour is drawn as a black dashed line, and the shading indicates the negative log-likelihood, with the scale shown on the right hand side of the plots.
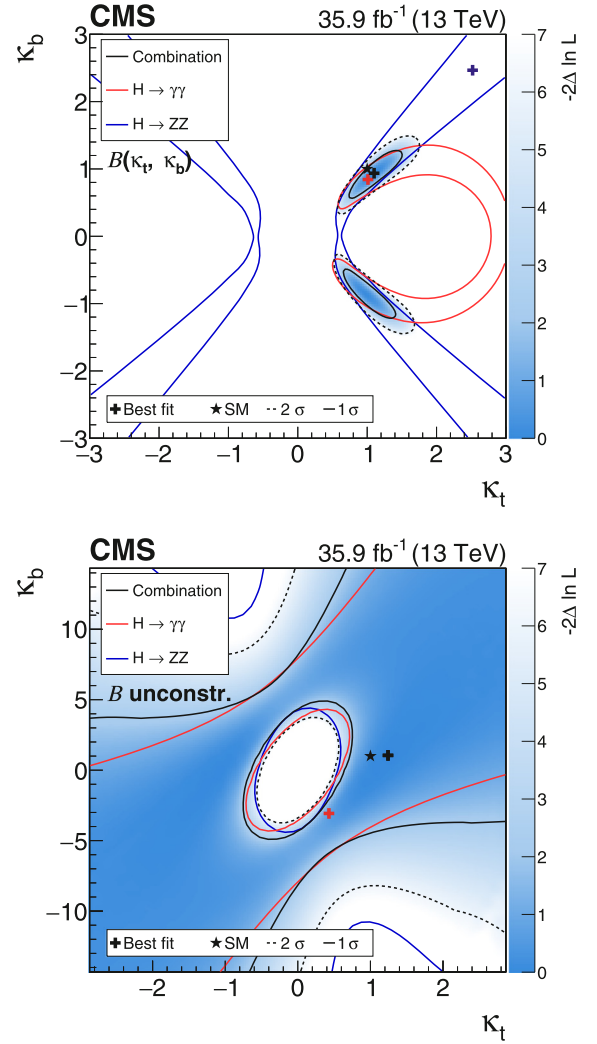
Fig. 10. Simultaneous fit to data for κ_t and κ_b, assuming a coupling dependence of the branching fractions (upper) and the branching fractions implemented as nuisance parameters with no prior constraint (lower). The one standard deviation contour is drawn for the combination ($H \to \gamma\gamma$, $H \to ZZ$, and $H \to b\bar{b}$), the $H \to \gamma\gamma$ channel, and the $H \to ZZ$ channel in black, red, and blue, respectively. For the combination the two standard deviation contour is drawn as a black dashed line, and the shading indicates the negative log-likelihood, with the scale shown on the right hand side of the plots.

the total cross section for Higgs boson production based on a combination of the $H \to \gamma\gamma$ and $H \to ZZ$ channels is measured to be $61.1 \pm 6.0\,(\text{stat}) \pm 3.7\,(\text{syst})\,\text{pb}$.

The spectra obtained are interpreted in the κ-framework [32], in which simultaneous variations of κ_b and κ_c, κ_t and κ_b, and κ_t and the anomalous direct coupling to the gluon field c_g are fitted to the p_T^H spectra. The limits obtained for the individual couplings are $-1.1 < \kappa_b < 1.1$ and $-4.9 < \kappa_c < 4.8$ at 95% confidence level, assuming the branching fractions scale with the Higgs boson couplings following the standard model prediction. For the charm coupling κ_c in particular, these bounds are comparable with those obtained from direct searches with charm quarks in the final state.

Acknowledgements

Appendix A. Tables for the differential cross section measurements

Tables A.1–A.5 show the measured differential cross sections for the considered observables.

Table A.1
Differential cross sections (pb/GeV) for the observable p_T^H.

p_T^H (GeV)	0–15	15–30	30–45	45–80	80–120	120–200	200–350	350–600	>600
H → γγ	$1.0^{+0.3}_{-0.3}$	$1^{+0.3}_{-0.3}$	$0.5^{+0.2}_{-0.2}$	$0.3^{+0.1}_{-0.1}$	$0.1^{+0.05}_{-0.05}$	$0.03^{+0.01}_{-0.01}$	$0.01^{+2.8\times10^{-3}}_{-2.5\times10^{-3}}$	$-3.4\times10^{-5}\,^{+3.8\times10^{-4}}_{-3.1\times10^{-4}}$	$-1.9\times10^{-4}\,^{+2.4\times10^{-4}}_{-2.4\times10^{-4}}$
H → ZZ	$0.7^{+0.3}_{-0.3}$	$1^{+0.4}_{-0.3}$	$0.4^{+0.1}_{-0.1}$		$0.08^{+0.03}_{-0.02}$		$3.3\times10^{-4}\,^{+2.6\times10^{-3}}_{-2.6\times10^{-3}}$		
H → b$\overline{\text{b}}$	*None*							$9.6\times10^{-4}\,^{+1.2\times10^{-3}}_{-1.2\times10^{-3}}$	$1.1\times10^{-4}\,^{+1.2\times10^{-4}}_{-1.1\times10^{-4}}$
Comb.	$0.8^{+0.2}_{-0.2}$	$1^{+0.2}_{-0.3}$	$0.6^{+0.2}_{-0.2}$	$0.3^{+0.1}_{-0.09}$	$0.1^{+0.05}_{-0.04}$	$0.03^{+0.01}_{-0.01}$	$0.01^{+2.6\times10^{-3}}_{-2.4\times10^{-3}}$	$-2.8\times10^{-6}\,^{+3.7\times10^{-4}}_{-2.8\times10^{-4}}$	$5.8\times10^{-5}\,^{+1.0\times10^{-4}}_{-1.0\times10^{-4}}$

Table A.2
Differential cross sections of gluon fusion (ggH) (pb/GeV) for the observable p_T^H, with non-ggH production modes fixed to their SM prediction.

p_T^H (GeV)	0–15	15–30	30–45	45–80	80–120	120–200	200–350	350–600	>600
Comb.	$0.8^{+0.2}_{-0.2}$	$1^{+0.2}_{-0.3}$	$0.5^{+0.2}_{-0.2}$	$0.2^{+0.1}_{-0.09}$	$0.1^{+0.05}_{-0.04}$	$0.02^{+0.01}_{-0.01}$	$8.3\times10^{-3}\,^{+2.6\times10^{-3}}_{-2.4\times10^{-3}}$	$-1.6\times10^{-4}\,^{+3.4\times10^{-4}}_{-2.6\times10^{-4}}$	$3.5\times10^{-5}\,^{+5.8\times10^{-5}}_{-5.7\times10^{-5}}$

Table A.3
Differential cross sections (pb) for the observable N_{jets}.

N_{jets}	0	1	2	3	≥4
H → γγ	$50^{+8.5}_{-8.1}$	$14^{+5.1}_{-4.9}$	$4.8\times10^{-1}\,^{+2.7}_{-2.7}$	$3.1^{+2.0}_{-2.0}$	$1.3^{+8.8\times10^{-1}}_{-9.3\times10^{-1}}$
H → ZZ	$41^{+9.1}_{-8.0}$	$8.7^{+5.2}_{-4.3}$	$6.9^{+3.7}_{-3.0}$	$1.2^{+2.1}_{-2.1}$	
Combination	$47^{+6.2}_{-6.4}$	$11^{+3.7}_{-3.4}$	$3.5^{+1.9}_{-1.7}$	$1.8^{+1.7}_{-1.5}$	$1.2^{+8.3\times10^{-1}}_{-8.8\times10^{-1}}$

Table A.4
Differential cross sections (pb) for the observable $|y_H|$.

$|y_H|$	0–0.15	0.15–0.3	0.3–0.6	0.6–0.9	0.9–1.2	1.2–2.5
H → γγ	42^{+11}_{-11}	39^{+12}_{-11}	$31^{+9.0}_{-7.5}$	$28^{+9.1}_{-8.7}$	24^{+12}_{-10}	$18^{+7.4}_{-7.2}$
H → ZZ	39^{+17}_{-14}	35^{+18}_{-14}	$34^{+11}_{-9.8}$	45^{+13}_{-11}	$13^{+8.9}_{-6.8}$	$13^{+6.7}_{-5.4}$
Combination	$41^{+9.1}_{-8.9}$	$38^{+9.7}_{-9.2}$	$32^{+7.0}_{-6.0}$	$35^{+7.1}_{-6.6}$	$17^{+7.4}_{-6.5}$	$15^{+5.1}_{-4.7}$

Table A.5
Differential cross sections (pb/GeV) for the observable p_T^{jet}.

p_T^{jet} (GeV)	30–55	55–95	95–120	120–200	>200
H → γγ	$1.6\times10^{-1}\,^{+2.0\times10^{-1}}_{-2.1\times10^{-1}}$	$2.0\times10^{-1}\,^{+9.2\times10^{-2}}_{-9.3\times10^{-2}}$	$1.3\times10^{-1}\,^{+9.5\times10^{-2}}_{-9.2\times10^{-2}}$	$1.5\times10^{-5}\,^{+1.8\times10^{-2}}_{-1.7\times10^{-2}}$	$2.9\times10^{-2}\,^{+9.1\times10^{-3}}_{-9.2\times10^{-3}}$
H → ZZ	$4.8\times10^{-1}\,^{+2.4\times10^{-1}}_{-2.0\times10^{-1}}$	$7.7\times10^{-2}\,^{+8.8\times10^{-2}}_{-6.9\times10^{-2}}$	$8.0\times10^{-2}\,^{+5.9\times10^{-2}}_{-4.4\times10^{-2}}$		
Combination	$3.2\times10^{-1}\,^{+1.4\times10^{-1}}_{-1.3\times10^{-1}}$	$1.3\times10^{-1}\,^{+7.7\times10^{-2}}_{-6.1\times10^{-2}}$	$1.1\times10^{-1}\,^{+8.4\times10^{-2}}_{-8.1\times10^{-2}}$	$-4.2\times10^{-3}\,^{+1.7\times10^{-2}}_{-1.6\times10^{-2}}$	$2.7\times10^{-2}\,^{+8.7\times10^{-3}}_{-8.9\times10^{-3}}$

Appendix B. Correlation matrices for the combinations of differential observables

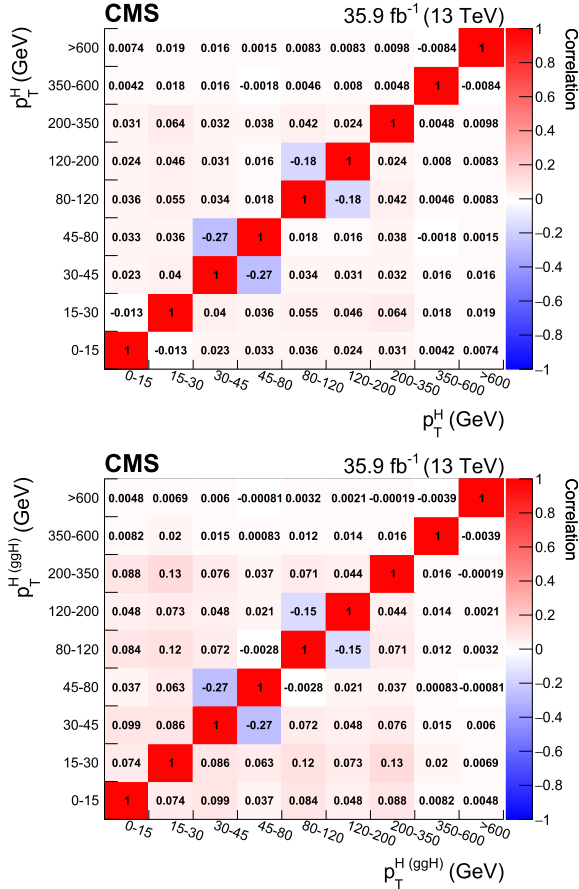Figs. B.1–B.4 show the correlation matrices for the considered observables.

Fig. B.1. Bin-to-bin correlation matrix of the p_T^H spectrum (upper) and of the p_T^H spectrum of gluon fusion (ggH), where the non-ggH contributions are fixed to the SM expectation (lower).
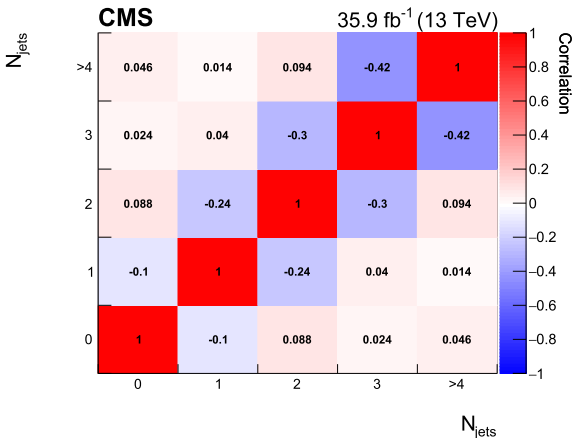

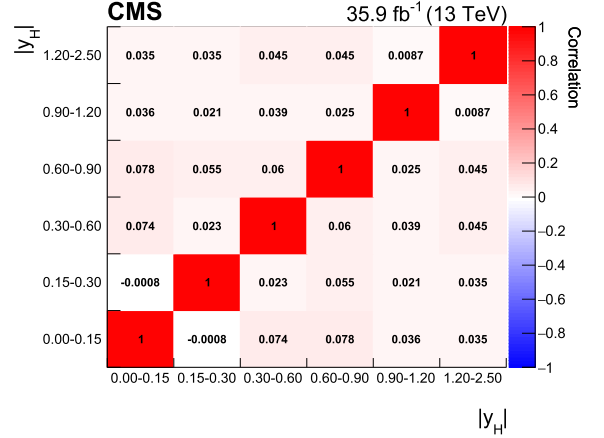**Fig. B.2.** Bin-to-bin correlation matrix of the N_{jets} spectrum.

Fig. B.3. Bin-to-bin correlation matrix of the $|y_H|$ spectrum.
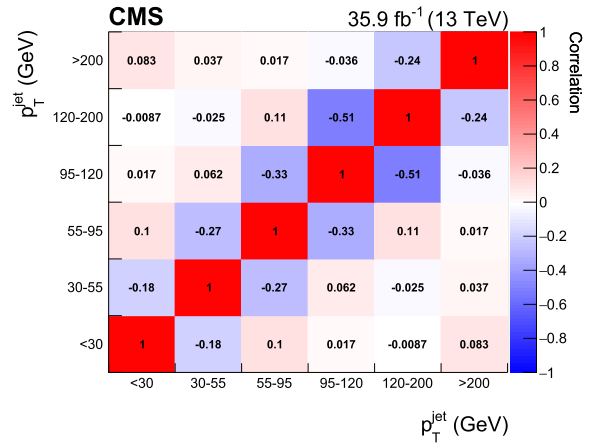
Fig. B.4. Bin-to-bin correlation matrix of the p_T^{jet} spectrum.

References

[1] P.W. Higgs, Broken symmetries and the masses of gauge bosons, Phys. Rev. Lett. 13 (1964) 508, https://doi.org/10.1103/PhysRevLett.13.508.

[2] F. Englert, R. Brout, Broken symmetry and the mass of gauge vector mesons, Phys. Rev. Lett. 13 (1964) 321, https://doi.org/10.1103/PhysRevLett.13.321.

[3] G.S. Guralnik, C.R. Hagen, T.W.B. Kibble, Global conservation laws and massless particles, Phys. Rev. Lett. 13 (1964) 585, https://doi.org/10.1103/PhysRevLett.13.585.

[4] ATLAS Collaboration, Observation of a new particle in the search for the standard model Higgs boson with the ATLAS detector at the LHC, Phys. Lett. B 716 (2012) 1, https://doi.org/10.1016/j.physletb.2012.08.020, arXiv:1207.7214.

[5] CMS Collaboration, Observation of a new boson at a mass of 125 GeV with the CMS experiment at the LHC, Phys. Lett. B 716 (2012) 30, https://doi.org/10.1016/j.physletb.2012.08.021, arXiv:1207.7235.

[6] CMS Collaboration, Observation of a new boson with mass near 125 GeV in pp collisions at $\sqrt{s} = 7$ and 8 TeV, J. High Energy Phys. 06 (2013) 081, https://doi.org/10.1007/JHEP06(2013)081, arXiv:1303.4571.

[7] ATLAS, CMS Collaborations, Measurements of the Higgs boson production and decay rates and constraints on its couplings from a combined ATLAS and CMS analysis of the LHC pp collision data at $\sqrt{s} = 7$ and 8 TeV, J. High Energy Phys. 08 (2016) 045, https://doi.org/10.1007/JHEP08(2016)045, arXiv:1606.02266.

[8] ATLAS, CMS Collaborations, Combined measurement of the Higgs boson mass in pp collisions at $\sqrt{s} = 7$ and 8 TeV with the ATLAS and CMS experiments, Phys. Rev. Lett. 114 (2015) 191803, https://doi.org/10.1103/PhysRevLett.114.191803, arXiv:1503.07589.

[9] CMS Collaboration, Combined measurements of Higgs boson couplings in proton-proton collisions at $\sqrt{s} = 13$ TeV, submitted to Eur. Phys. J. C (2018), arXiv:1809.10733.

[10] S. Dimopoulos, H. Georgi, Softly broken supersymmetry and SU(5), Nucl. Phys. B 193 (1981) 150, https://doi.org/10.1016/0550-3213(81)90522-8.

[11] E. Witten, Dynamical breaking of supersymmetry, Nucl. Phys. B 188 (1981) 513, https://doi.org/10.1016/0550-3213(81)90006-7.

[12] F. Bishara, U. Haisch, P.F. Monni, E. Re, Constraining light-quark Yukawa couplings from Higgs distributions, Phys. Rev. Lett. 118 (2017) 121801, https://doi.org/10.1103/PhysRevLett.118.121801, arXiv:1606.09253.

[13] ATLAS Collaboration, Measurements of the total and differential Higgs boson production cross sections combining the H → γγ and H → ZZ → 4ℓ decay channels at √s = 8 TeV with the ATLAS detector, Phys. Rev. Lett. 115 (2015) 091801, https://doi.org/10.1103/PhysRevLett.115.091801, arXiv:1504.05833.

[14] ATLAS Collaboration, Search for Higgs and Z boson decays to J/ψγ and Υ(nS)γ with the ATLAS detector, Phys. Rev. Lett. 114 (2015) 121801, https://doi.org/10.1103/PhysRevLett.114.121801, arXiv:1501.03276.

[15] M. König, M. Neubert, Exclusive radiative Higgs decays as probes of light-quark Yukawa couplings, J. High Energy Phys. 08 (2015) 012, https://doi.org/10.1007/JHEP08(2015)012, arXiv:1505.03870.

[16] ATLAS Collaboration, Searches for exclusive Higgs and Z boson decays into J/ψγ, ψ(2S)γ, and Υ(nS)γ at √s = 13 TeV with the ATLAS detector, Phys. Lett. B 786 (2018) 134, https://doi.org/10.1016/j.physletb.2018.09.024, arXiv:1807.00802.

[17] ATLAS Collaboration, Search for the decay of the Higgs boson to charm quarks with the ATLAS experiment, Phys. Rev. Lett. 120 (2018) 211802, https://doi.org/10.1103/PhysRevLett.120.211802, arXiv:1802.04329.

[18] ATLAS Collaboration, Measurements of fiducial and differential cross sections for Higgs boson production in the diphoton decay channel at √s = 8 TeV with ATLAS, J. High Energy Phys. 09 (2014) 112, https://doi.org/10.1007/JHEP09(2014)112, arXiv:1407.4222.

[19] CMS Collaboration, Measurement of differential cross sections for Higgs boson production in the diphoton decay channel in pp collisions at √s = 8 TeV, Eur. Phys. J. C 76 (2016) 13, https://doi.org/10.1140/epjc/s10052-015-3853-3, arXiv:1508.07819.

[20] ATLAS Collaboration, Fiducial and differential cross sections of Higgs boson production measured in the four-lepton decay channel in pp collisions at √s = 8 TeV with the ATLAS detector, Phys. Lett. B 738 (2014) 234, https://doi.org/10.1016/j.physletb.2014.09.054, arXiv:1408.3226.

[21] CMS Collaboration, Measurement of differential and integrated fiducial cross sections for Higgs boson production in the four-lepton decay channel in pp collisions at √s = 7 and 8 TeV, J. High Energy Phys. 04 (2016) 005, https://doi.org/10.1007/JHEP04(2016)005, arXiv:1512.08377.

[22] ATLAS Collaboration, Measurement of fiducial differential cross sections of gluon-fusion production of Higgs bosons decaying to WW* → eνμν with the ATLAS detector at √s = 8 TeV, J. High Energy Phys. 08 (2016) 104, https://doi.org/10.1007/JHEP08(2016)104, arXiv:1604.02997.

[23] CMS Collaboration, Measurement of the transverse momentum spectrum of the Higgs boson produced in pp collisions at √s = 8 TeV using H → WW decays, J. High Energy Phys. 03 (2017) 032, https://doi.org/10.1007/JHEP03(2017)032, arXiv:1606.01522.

[24] ATLAS Collaboration, Measurements of Higgs boson properties in the diphoton decay channel with 36 fb⁻¹ of pp collision data at √s = 13 TeV with the ATLAS detector, Phys. Rev. D 98 (2018) 052005, https://doi.org/10.1103/PhysRevD.98.052005, arXiv:1802.04146.

[25] CMS Collaboration, Measurement of inclusive and differential Higgs boson production cross sections in the diphoton decay channel in proton-proton collisions at √s = 13 TeV, J. High Energy Phys. 01 (2019) 183, https://doi.org/10.1007/JHEP01(2019)183, arXiv:1807.03825.

[26] ATLAS Collaboration, Measurement of inclusive and differential cross sections in the H → ZZ* → 4ℓ decay channel in pp collisions at √s = 13 TeV with the ATLAS detector, J. High Energy Phys. 10 (2017) 132, https://doi.org/10.1007/JHEP10(2017)132, arXiv:1708.02810.

[27] CMS Collaboration, Measurements of properties of the Higgs boson decaying into the four-lepton final state in pp collisions at √s = 13 TeV, J. High Energy Phys. 11 (2017) 047, https://doi.org/10.1007/JHEP11(2017)047, arXiv:1706.09936.

[28] ATLAS Collaboration, Combined measurement of differential and total cross sections in the H → γγ and the H → ZZ* → 4ℓ decay channels at √s = 13 TeV with the ATLAS detector, Phys. Lett. B 786 (2018) 114, https://doi.org/10.1016/j.physletb.2018.09.019, arXiv:1805.10197.

[29] CMS Collaboration, Inclusive search for a highly boosted Higgs boson decaying to a bottom quark-antiquark pair, Phys. Rev. Lett. 120 (2018) 071802, https://doi.org/10.1103/PhysRevLett.120.071802, arXiv:1709.05543.

[30] M. Grazzini, A. Ilnicka, M. Spira, M. Wiesemann, Effective field theory for Higgs properties parametrisation: the transverse momentum spectrum case, in: Proceedings, 52nd Rencontres de Moriond on QCD and High Energy Interactions, La Thuile, Italy, March 25-April 1, 2017, 2017, p. 23, https://inspirehep.net/record/1599583/files/1705.05143.pdf, arXiv:1705.05143.

[31] M. Grazzini, A. Ilnicka, M. Spira, M. Wiesemann, Modeling BSM effects on the Higgs transverse-momentum spectrum in an EFT approach, J. High Energy Phys. 03 (2017) 115, https://doi.org/10.1007/JHEP03(2017)115, arXiv:1612.00283.

[32] LHC Higgs Cross Section Working Group, Handbook of LHC Higgs cross sections: 3. Higgs properties, CERN, https://doi.org/10.5170/CERN-2013-004, arXiv:1307.1347, 2013.

[33] A. Banfi, P.F. Monni, G. Zanderighi, Quark masses in Higgs production with a jet veto, J. High Energy Phys. 01 (2014) 097, https://doi.org/10.1007/JHEP01(2014)097, arXiv:1308.4634.

[34] G. Bozzi, S. Catani, D. de Florian, M. Grazzini, The qₜ spectrum of the Higgs boson at the LHC in QCD perturbation theory, Phys. Lett. B 564 (2003) 65, https://doi.org/10.1016/S0370-2693(03)00656-7, arXiv:hep-ph/0302104.

[35] T. Becher, M. Neubert, Drell-Yan production at small qₜ, transverse parton distributions and the collinear anomaly, Eur. Phys. J. C 71 (2011) 1665, https://doi.org/10.1140/epjc/s10052-011-1665-7, arXiv:1007.4005.

[36] P.F. Monni, E. Re, P. Torrielli, Higgs transverse-momentum resummation in direct space, Phys. Rev. Lett. 116 (2016) 242001, https://doi.org/10.1103/PhysRevLett.116.242001, arXiv:1604.02191.

[37] CMS Collaboration, The CMS experiment at the CERN LHC, J. Instrum. 3 (2008) S08004, https://doi.org/10.1088/1748-0221/3/08/S08004.

[38] J. Alwall, R. Frederix, S. Frixione, V. Hirschi, F. Maltoni, O. Mattelaer, H.S. Shao, T. Stelzer, P. Torrielli, M. Zaro, The automated computation of tree-level and next-to-leading order differential cross sections, and their matching to parton shower simulations, J. High Energy Phys. 07 (2014) 079, https://doi.org/10.1007/JHEP07(2014)079, arXiv:1405.0301.

[39] T. Sjöstrand, S. Ask, J.R. Christiansen, R. Corke, N. Desai, P. Ilten, S. Mrenna, S. Prestel, C.O. Rasmussen, P.Z. Skands, An introduction to PYTHIA 8.2, Comput. Phys. Commun. 191 (2015) 159, https://doi.org/10.1016/j.cpc.2015.01.024, arXiv:1410.3012.

[40] P. Skands, S. Carrazza, J. Rojo, Tuning PYTHIA 8.1: the Monash 2013 tune, Eur. Phys. J. C 74 (2014) 3024, https://doi.org/10.1140/epjc/s10052-014-3024-y, arXiv:1404.5630.

[41] R. Frederix, S. Frixione, Merging meets matching in MC@NLO, J. High Energy Phys. 12 (2012) 061, https://doi.org/10.1007/JHEP12(2012)061, arXiv:1209.6215.

[42] K. Hamilton, P. Nason, G. Zanderighi, MINLO: multi-scale improved NLO, J. High Energy Phys. 10 (2012) 155, https://doi.org/10.1007/JHEP10(2012)155, arXiv:1206.3572.

[43] A. Kardos, P. Nason, C. Oleari, Three-jet production in POWHEG, J. High Energy Phys. 04 (2014) 043, https://doi.org/10.1007/JHEP04(2014)043, arXiv:1402.4001.

[44] R.D. Ball, et al., NNPDF, Parton distributions for the LHC Run II, J. High Energy Phys. 04 (2015) 040, https://doi.org/10.1007/JHEP04(2015)040, arXiv:1410.8849.

[45] CMS Collaboration, Particle-flow reconstruction and global event description with the CMS detector, J. Instrum. 12 (2017) P10003, https://doi.org/10.1088/1748-0221/12/10/P10003, arXiv:1706.04965.

[46] M. Cacciari, G.P. Salam, G. Soyez, The anti-kₜ jet clustering algorithm, J. High Energy Phys. 04 (2008) 063, https://doi.org/10.1088/1126-6708/2008/04/063, arXiv:0802.1189.

[47] M. Dasgupta, A. Fregoso, S. Marzani, G.P. Salam, Towards an understanding of jet substructure, J. High Energy Phys. 09 (2013) 029, https://doi.org/10.1007/JHEP09(2013)029, arXiv:1307.0007.

[48] A.J. Larkoski, S. Marzani, G. Soyez, J. Thaler, Soft drop, J. High Energy Phys. 05 (2014) 146, https://doi.org/10.1007/JHEP05(2014)146, arXiv:1402.2657.

[49] J. Dolen, P. Harris, S. Marzani, S. Rappoccio, N. Tran, Thinking outside the ROCs: designing decorrelated taggers (DDT) for jet substructure, J. High Energy Phys. 05 (2016) 156, https://doi.org/10.1007/JHEP05(2016)156, arXiv:1603.00027.

[50] I. Moult, L. Necib, J. Thaler, New angles on energy correlation functions, J. High Energy Phys. 12 (2016) 153, https://doi.org/10.1007/JHEP12(2016)153, arXiv:1609.07483.

[51] A.J. Larkoski, G.P. Salam, J. Thaler, Energy correlation functions for jet substructure, J. High Energy Phys. 06 (2013) 108, https://doi.org/10.1007/JHEP06(2013)108, arXiv:1305.0007.

[52] J. Thaler, K. Van Tilburg, Identifying boosted objects with N-subjettiness, J. High Energy Phys. 03 (2011) 015, https://doi.org/10.1007/JHEP03(2011)015, arXiv:1011.2268.

[53] CMS Collaboration, Identification of heavy-flavour jets with the CMS detector in pp collisions at 13 TeV, J. Instrum. 13 (2018) P05011, https://doi.org/10.1088/1748-0221/13/05/P05011, arXiv:1712.07158.

[54] P.C. Hansen, The L-curve and its use in the numerical treatment of inverse problems, in: Computational Inverse Problems in Electrocardiology, WIT Press, Southampton, 2001, p. 119, https://www.sintef.no/globalassets/project/evitameeting/2005/lcurve.pdf.

[55] G. Cowan, K. Cranmer, E. Gross, O. Vitells, Asymptotic formulae for likelihood-based tests of new physics, Eur. Phys. J. C 71 (2011) 1554, https://doi.org/10.1140/epjc/s10052-011-1554-0, arXiv:1007.1727, Erratum: https://doi.org/10.1140/epjc/s10052-013-2501-z.

[56] The ATLAS Collaboration, The CMS Collaboration, The LHC Higgs Combination Group, Procedure for the LHC Higgs Boson Search Combination in Summer 2011, Technical Report CMS-NOTE-2011-005, ATL-PHYS-PUB-2011-11, 2011, https://cds.cern.ch/record/1379837.

[57] LHC Higgs Cross Section Working Group, Handbook of LHC Higgs cross sections: 4. Deciphering the nature of the Higgs sector, CERN, https://doi.org/10.23731/CYRM-2017-002, arXiv:1610.07922, 2016.

The CMS Collaboration

A.M. Sirunyan, A. Tumasyan

Yerevan Physics Institute, Yerevan, Armenia

W. Adam, F. Ambrogi, E. Asilar, T. Bergauer, J. Brandstetter, M. Dragicevic, J. Erö, A. Escalante Del Valle, M. Flechl, R. Frühwirth [1], V.M. Ghete, J. Hrubec, M. Jeitler [1], N. Krammer, I. Krätschmer, D. Liko, T. Madlener, I. Mikulec, N. Rad, H. Rohringer, J. Schieck [1], R. Schöfbeck, M. Spanring, D. Spitzbart, A. Taurok, W. Waltenberger, J. Wittmann, C.-E. Wulz [1], M. Zarucki

Institut für Hochenergiephysik, Wien, Austria

V. Chekhovsky, V. Mossolov, J. Suarez Gonzalez

Institute for Nuclear Problems, Minsk, Belarus

E.A. De Wolf, D. Di Croce, X. Janssen, J. Lauwers, M. Pieters, H. Van Haevermaet, P. Van Mechelen, N. Van Remortel

Universiteit Antwerpen, Antwerpen, Belgium

S. Abu Zeid, F. Blekman, J. D'Hondt, J. De Clercq, K. Deroover, G. Flouris, D. Lontkovskyi, S. Lowette, I. Marchesini, S. Moortgat, L. Moreels, Q. Python, K. Skovpen, S. Tavernier, W. Van Doninck, P. Van Mulders, I. Van Parijs

Vrije Universiteit Brussel, Brussel, Belgium

D. Beghin, B. Bilin, H. Brun, B. Clerbaux, G. De Lentdecker, H. Delannoy, B. Dorney, G. Fasanella, L. Favart, R. Goldouzian, A. Grebenyuk, A.K. Kalsi, T. Lenzi, J. Luetic, N. Postiau, E. Starling, L. Thomas, C. Vander Velde, P. Vanlaer, D. Vannerom, Q. Wang

Université Libre de Bruxelles, Bruxelles, Belgium

T. Cornelis, D. Dobur, A. Fagot, M. Gul, I. Khvastunov [2], D. Poyraz, C. Roskas, D. Trocino, M. Tytgat, W. Verbeke, B. Vermassen, M. Vit, N. Zaganidis

Ghent University, Ghent, Belgium

H. Bakhshiansohi, O. Bondu, S. Brochet, G. Bruno, C. Caputo, P. David, C. Delaere, M. Delcourt, A. Giammanco, G. Krintiras, V. Lemaitre, A. Magitteri, K. Piotrzkowski, A. Saggio, M. Vidal Marono, S. Wertz, J. Zobec

Université Catholique de Louvain, Louvain-la-Neuve, Belgium

F.L. Alves, G.A. Alves, M. Correa Martins Junior, G. Correia Silva, C. Hensel, A. Moraes, M.E. Pol, P. Rebello Teles

Centro Brasileiro de Pesquisas Fisicas, Rio de Janeiro, Brazil

E. Belchior Batista Das Chagas, W. Carvalho, J. Chinellato [3], E. Coelho, E.M. Da Costa, G.G. Da Silveira [4], D. De Jesus Damiao, C. De Oliveira Martins, S. Fonseca De Souza, H. Malbouisson, D. Matos Figueiredo, M. Melo De Almeida, C. Mora Herrera, L. Mundim, H. Nogima, W.L. Prado Da Silva, L.J. Sanchez Rosas, A. Santoro, A. Sznajder, M. Thiel, E.J. Tonelli Manganote [3], F. Torres Da Silva De Araujo, A. Vilela Pereira

Universidade do Estado do Rio de Janeiro, Rio de Janeiro, Brazil

S. Ahuja [a], C.A. Bernardes [a], L. Calligaris [a], T.R. Fernandez Perez Tomei [a], E.M. Gregores [b], P.G. Mercadante [b], S.F. Novaes [a], S.S. Padula [a]

[a] *Universidade Estadual Paulista, São Paulo, Brazil*
[b] *Universidade Federal do ABC, São Paulo, Brazil*

A. Aleksandrov, R. Hadjiiska, P. Iaydjiev, A. Marinov, M. Misheva, M. Rodozov, M. Shopova, G. Sultanov

Institute for Nuclear Research and Nuclear Energy, Bulgarian Academy of Sciences, Sofia, Bulgaria

A. Dimitrov, L. Litov, B. Pavlov, P. Petkov

University of Sofia, Sofia, Bulgaria

W. Fang [5], X. Gao [5], L. Yuan

Beihang University, Beijing, China

M. Ahmad, J.G. Bian, G.M. Chen, H.S. Chen, M. Chen, Y. Chen, C.H. Jiang, D. Leggat, H. Liao, Z. Liu, F. Romeo, S.M. Shaheen [6], A. Spiezia, J. Tao, Z. Wang, E. Yazgan, H. Zhang, S. Zhang [6], J. Zhao

Institute of High Energy Physics, Beijing, China

Y. Ban, G. Chen, A. Levin, J. Li, L. Li, Q. Li, Y. Mao, S.J. Qian, D. Wang

State Key Laboratory of Nuclear Physics and Technology, Peking University, Beijing, China

Y. Wang

Tsinghua University, Beijing, China

C. Avila, A. Cabrera, C.A. Carrillo Montoya, L.F. Chaparro Sierra, C. Florez, C.F. González Hernández, M.A. Segura Delgado

Universidad de Los Andes, Bogota, Colombia

B. Courbon, N. Godinovic, D. Lelas, I. Puljak, T. Sculac

University of Split, Faculty of Electrical Engineering, Mechanical Engineering and Naval Architecture, Split, Croatia

Z. Antunovic, M. Kovac

University of Split, Faculty of Science, Split, Croatia

V. Brigljevic, D. Ferencek, K. Kadija, B. Mesic, A. Starodumov [7], T. Susa

Institute Rudjer Boskovic, Zagreb, Croatia

M.W. Ather, A. Attikis, M. Kolosova, G. Mavromanolakis, J. Mousa, C. Nicolaou, F. Ptochos, P.A. Razis, H. Rykaczewski

University of Cyprus, Nicosia, Cyprus

M. Finger [8], M. Finger Jr. [8]

Charles University, Prague, Czech Republic

E. Ayala

Escuela Politecnica Nacional, Quito, Ecuador

E. Carrera Jarrin

Universidad San Francisco de Quito, Quito, Ecuador

H. Abdalla [9], A.A. Abdelalim [10,11], A. Mohamed [11]

Academy of Scientific Research and Technology of the Arab Republic of Egypt, Egyptian Network of High Energy Physics, Cairo, Egypt

S. Bhowmik, A. Carvalho Antunes De Oliveira, R.K. Dewanjee, K. Ehataht, M. Kadastik, M. Raidal, C. Veelken

National Institute of Chemical Physics and Biophysics, Tallinn, Estonia

P. Eerola, H. Kirschenmann, J. Pekkanen, M. Voutilainen

Department of Physics, University of Helsinki, Helsinki, Finland

J. Havukainen, J.K. Heikkilä, T. Järvinen, V. Karimäki, R. Kinnunen, T. Lampén, K. Lassila-Perini, S. Laurila, S. Lehti, T. Lindén, P. Luukka, T. Mäenpää, H. Siikonen, E. Tuominen, J. Tuominiemi

Helsinki Institute of Physics, Helsinki, Finland

T. Tuuva

Lappeenranta University of Technology, Lappeenranta, Finland

M. Besancon, F. Couderc, M. Dejardin, D. Denegri, J.L. Faure, F. Ferri, S. Ganjour, A. Givernaud, P. Gras, G. Hamel de Monchenault, P. Jarry, C. Leloup, E. Locci, J. Malcles, G. Negro, J. Rander, A. Rosowsky, M.Ö. Sahin, M. Titov

IRFU, CEA, Université Paris-Saclay, Gif-sur-Yvette, France

A. Abdulsalam [12], C. Amendola, I. Antropov, F. Beaudette, P. Busson, C. Charlot, R. Granier de Cassagnac, I. Kucher, A. Lobanov, J. Martin Blanco, C. Martin Perez, M. Nguyen, C. Ochando, G. Ortona, P. Paganini, P. Pigard, J. Rembser, R. Salerno, J.B. Sauvan, Y. Sirois, A.G. Stahl Leiton, A. Zabi, A. Zghiche

Laboratoire Leprince-Ringuet, Ecole polytechnique, CNRS/IN2P3, Université Paris-Saclay, Palaiseau, France

J.-L. Agram [13], J. Andrea, D. Bloch, J.-M. Brom, E.C. Chabert, V. Cherepanov, C. Collard, E. Conte [13], J.-C. Fontaine [13], D. Gelé, U. Goerlach, M. Jansová, A.-C. Le Bihan, N. Tonon, P. Van Hove

Université de Strasbourg, CNRS, IPHC UMR 7178, Strasbourg, France

S. Gadrat

Centre de Calcul de l'Institut National de Physique Nucleaire et de Physique des Particules, CNRS/IN2P3, Villeurbanne, France

S. Beauceron, C. Bernet, G. Boudoul, N. Chanon, R. Chierici, D. Contardo, P. Depasse, H. El Mamouni, J. Fay, L. Finco, S. Gascon, M. Gouzevitch, G. Grenier, B. Ille, F. Lagarde, I.B. Laktineh, H. Lattaud, M. Lethuillier, L. Mirabito, S. Perries, A. Popov [14], V. Sordini, G. Touquet, M. Vander Donckt, S. Viret

Université de Lyon, Université Claude Bernard Lyon 1, CNRS-IN2P3, Institut de Physique Nucléaire de Lyon, Villeurbanne, France

A. Khvedelidze [8]

Georgian Technical University, Tbilisi, Georgia

Z. Tsamalaidze [8]

Tbilisi State University, Tbilisi, Georgia

C. Autermann, L. Feld, M.K. Kiesel, K. Klein, M. Lipinski, M. Preuten, M.P. Rauch, C. Schomakers, J. Schulz, M. Teroerde, B. Wittmer

RWTH Aachen University, I. Physikalisches Institut, Aachen, Germany

A. Albert, D. Duchardt, M. Erdmann, S. Erdweg, T. Esch, R. Fischer, S. Ghosh, A. Güth, T. Hebbeker, C. Heidemann, K. Hoepfner, H. Keller, L. Mastrolorenzo, M. Merschmeyer, A. Meyer, P. Millet, S. Mukherjee, T. Pook, M. Radziej, H. Reithler, M. Rieger, A. Schmidt, D. Teyssier, S. Thüer

RWTH Aachen University, III. Physikalisches Institut A, Aachen, Germany

G. Flügge, O. Hlushchenko, T. Kress, T. Müller, A. Nehrkorn, A. Nowack, C. Pistone, O. Pooth, D. Roy, H. Sert, A. Stahl [15]

RWTH Aachen University, III. Physikalisches Institut B, Aachen, Germany

M. Aldaya Martin, T. Arndt, C. Asawatangtrakuldee, I. Babounikau, K. Beernaert, O. Behnke, U. Behrens, A. Bermúdez Martínez, D. Bertsche, A.A. Bin Anuar, K. Borras [16], V. Botta, A. Campbell, P. Connor, C. Contreras-Campana, V. Danilov, A. De Wit, M.M. Defranchis, C. Diez Pardos, D. Domínguez Damiani, G. Eckerlin, T. Eichhorn, A. Elwood, E. Eren, E. Gallo [17], A. Geiser, J.M. Grados Luyando, A. Grohsjean, M. Guthoff, M. Haranko, A. Harb, J. Hauk, H. Jung, M. Kasemann, J. Keaveney, C. Kleinwort, J. Knolle, D. Krücker, W. Lange, A. Lelek, T. Lenz, J. Leonard, K. Lipka, W. Lohmann [18], R. Mankel, I.-A. Melzer-Pellmann, A.B. Meyer, M. Meyer, M. Missiroli, G. Mittag, J. Mnich, V. Myronenko, S.K. Pflitsch, D. Pitzl, A. Raspereza, M. Savitskyi, P. Saxena, P. Schütze, C. Schwanenberger, R. Shevchenko, A. Singh, H. Tholen, O. Turkot, A. Vagnerini, G.P. Van Onsem, R. Walsh, Y. Wen, K. Wichmann, C. Wissing, O. Zenaiev

Deutsches Elektronen-Synchrotron, Hamburg, Germany

R. Aggleton, S. Bein, L. Benato, A. Benecke, V. Blobel, T. Dreyer, A. Ebrahimi, E. Garutti, D. Gonzalez, P. Gunnellini, J. Haller, A. Hinzmann, A. Karavdina, G. Kasieczka, R. Klanner, R. Kogler, N. Kovalchuk, S. Kurz, V. Kutzner, J. Lange, D. Marconi, J. Multhaup, M. Niedziela, C.E.N. Niemeyer, D. Nowatschin, A. Perieanu, A. Reimers, O. Rieger, C. Scharf, P. Schleper, S. Schumann, J. Schwandt, J. Sonneveld, H. Stadie, G. Steinbrück, F.M. Stober, M. Stöver, A. Vanhoefer, B. Vormwald, I. Zoi

University of Hamburg, Hamburg, Germany

M. Akbiyik, C. Barth, M. Baselga, S. Baur, E. Butz, R. Caspart, T. Chwalek, F. Colombo, W. De Boer, A. Dierlamm, K. El Morabit, N. Faltermann, B. Freund, M. Giffels, M.A. Harrendorf, F. Hartmann [15], S.M. Heindl, U. Husemann, I. Katkov [14], S. Kudella, S. Mitra, M.U. Mozer, Th. Müller, M. Musich, M. Plagge, G. Quast, K. Rabbertz, M. Schröder, I. Shvetsov, H.J. Simonis, R. Ulrich, S. Wayand, M. Weber, T. Weiler, C. Wöhrmann, R. Wolf

Karlsruher Institut fuer Technologie, Karlsruhe, Germany

G. Anagnostou, G. Daskalakis, T. Geralis, A. Kyriakis, D. Loukas, G. Paspalaki

Institute of Nuclear and Particle Physics (INPP), NCSR Demokritos, Aghia Paraskevi, Greece

G. Karathanasis, P. Kontaxakis, A. Panagiotou, I. Papavergou, N. Saoulidou, E. Tziaferi, K. Vellidis

National and Kapodistrian University of Athens, Athens, Greece

K. Kousouris, I. Papakrivopoulos, G. Tsipolitis

National Technical University of Athens, Athens, Greece

I. Evangelou, C. Foudas, P. Gianneios, P. Katsoulis, P. Kokkas, S. Mallios, N. Manthos, I. Papadopoulos, E. Paradas, J. Strologas, F.A. Triantis, D. Tsitsonis

University of Ioánnina, Ioánnina, Greece

M. Bartók [19], M. Csanad, N. Filipovic, P. Major, M.I. Nagy, G. Pasztor, O. Surányi, G.I. Veres

MTA-ELTE Lendület CMS Particle and Nuclear Physics Group, Eötvös Loránd University, Budapest, Hungary

G. Bencze, C. Hajdu, D. Horvath [20], Á. Hunyadi, F. Sikler, T.Á. Vámi, V. Veszpremi, G. Vesztergombi [†]

Wigner Research Centre for Physics, Budapest, Hungary

N. Beni, S. Czellar, J. Karancsi [19], A. Makovec, J. Molnar, Z. Szillasi

Institute of Nuclear Research ATOMKI, Debrecen, Hungary

P. Raics, Z.L. Trocsanyi, B. Ujvari

Institute of Physics, University of Debrecen, Debrecen, Hungary

S. Choudhury, J.R. Komaragiri, P.C. Tiwari

Indian Institute of Science (IISc), Bangalore, India

S. Bahinipati [21], C. Kar, P. Mal, K. Mandal, A. Nayak [22], D.K. Sahoo [21], S.K. Swain

National Institute of Science Education and Research, HBNI, Bhubaneswar, India

S. Bansal, S.B. Beri, V. Bhatnagar, S. Chauhan, R. Chawla, N. Dhingra, R. Gupta, A. Kaur, M. Kaur, S. Kaur, P. Kumari, M. Lohan, A. Mehta, K. Sandeep, S. Sharma, J.B. Singh, A.K. Virdi, G. Walia

Panjab University, Chandigarh, India

A. Bhardwaj, B.C. Choudhary, R.B. Garg, M. Gola, S. Keshri, Ashok Kumar, S. Malhotra, M. Naimuddin, P. Priyanka, K. Ranjan, Aashaq Shah, R. Sharma

University of Delhi, Delhi, India

R. Bhardwaj [23], M. Bharti [23], R. Bhattacharya, S. Bhattacharya, U. Bhawandeep [23], D. Bhowmik, S. Dey, S. Dutt [23], S. Dutta, S. Ghosh, K. Mondal, S. Nandan, A. Purohit, P.K. Rout, A. Roy, S. Roy Chowdhury, G. Saha, S. Sarkar, M. Sharan, B. Singh [23], S. Thakur [23]

Saha Institute of Nuclear Physics, HBNI, Kolkata, India

P.K. Behera

Indian Institute of Technology Madras, Madras, India

R. Chudasama, D. Dutta, V. Jha, V. Kumar, P.K. Netrakanti, L.M. Pant, P. Shukla

Bhabha Atomic Research Centre, Mumbai, India

T. Aziz, M.A. Bhat, S. Dugad, G.B. Mohanty, N. Sur, B. Sutar, R.K. Verma

Tata Institute of Fundamental Research-A, Mumbai, India

S. Banerjee, S. Bhattacharya, S. Chatterjee, P. Das, M. Guchait, Sa. Jain, S. Karmakar, S. Kumar, M. Maity [24], G. Majumder, K. Mazumdar, N. Sahoo, T. Sarkar [24]

Tata Institute of Fundamental Research-B, Mumbai, India

S. Chauhan, S. Dube, V. Hegde, A. Kapoor, K. Kothekar, S. Pandey, A. Rane, A. Rastogi, S. Sharma

Indian Institute of Science Education and Research (IISER), Pune, India

S. Chenarani [25], E. Eskandari Tadavani, S.M. Etesami [25], M. Khakzad, M. Mohammadi Najafabadi, M. Naseri, F. Rezaei Hosseinabadi, B. Safarzadeh [26], M. Zeinali

Institute for Research in Fundamental Sciences (IPM), Tehran, Iran

M. Felcini, M. Grunewald

University College Dublin, Dublin, Ireland

M. Abbrescia [a,b], C. Calabria [a,b], A. Colaleo [a], D. Creanza [a,c], L. Cristella [a,b], N. De Filippis [a,c], M. De Palma [a,b], A. Di Florio [a,b], F. Errico [a,b], L. Fiore [a], A. Gelmi [a,b], G. Iaselli [a,c], M. Ince [a,b], S. Lezki [a,b], G. Maggi [a,c], M. Maggi [a], G. Miniello [a,b], S. My [a,b], S. Nuzzo [a,b], A. Pompili [a,b], G. Pugliese [a,c], R. Radogna [a], A. Ranieri [a], G. Selvaggi [a,b], A. Sharma [a], L. Silvestris [a], R. Venditti [a], P. Verwilligen [a], G. Zito [a]

[a] *INFN Sezione di Bari, Bari, Italy*
[b] *Università di Bari, Bari, Italy*
[c] *Politecnico di Bari, Bari, Italy*

G. Abbiendi [a], C. Battilana [a,b], D. Bonacorsi [a,b], L. Borgonovi [a,b], S. Braibant-Giacomelli [a,b], R. Campanini [a,b], P. Capiluppi [a,b], A. Castro [a,b], F.R. Cavallo [a], S.S. Chhibra [a,b], C. Ciocca [a], G. Codispoti [a,b], M. Cuffiani [a,b], G.M. Dallavalle [a], F. Fabbri [a], A. Fanfani [a,b], E. Fontanesi, P. Giacomelli [a], C. Grandi [a], L. Guiducci [a,b], F. Iemmi [a,b], S. Lo Meo [a], S. Marcellini [a], G. Masetti [a], A. Montanari [a], F.L. Navarria [a,b], A. Perrotta [a], F. Primavera [a,b,15], T. Rovelli [a,b], G.P. Siroli [a,b], N. Tosi [a]

[a] *INFN Sezione di Bologna, Bologna, Italy*
[b] *Università di Bologna, Bologna, Italy*

S. Albergo [a,b], A. Di Mattia [a], R. Potenza [a,b], A. Tricomi [a,b], C. Tuve [a,b]

[a] *INFN Sezione di Catania, Catania, Italy*
[b] *Università di Catania, Catania, Italy*

G. Barbagli [a], K. Chatterjee [a,b], V. Ciulli [a,b], C. Civinini [a], R. D'Alessandro [a,b], E. Focardi [a,b], G. Latino,
P. Lenzi [a,b], M. Meschini [a], S. Paoletti [a], L. Russo [a,27], G. Sguazzoni [a], D. Strom [a], L. Viliani [a]

[a] *INFN Sezione di Firenze, Firenze, Italy*
[b] *Università di Firenze, Firenze, Italy*

L. Benussi, S. Bianco, F. Fabbri, D. Piccolo

INFN Laboratori Nazionali di Frascati, Frascati, Italy

F. Ferro [a], R. Mulargia [a,b], F. Ravera [a,b], E. Robutti [a], S. Tosi [a,b]

[a] *INFN Sezione di Genova, Genova, Italy*
[b] *Università di Genova, Genova, Italy*

A. Benaglia [a], A. Beschi [b], F. Brivio [a,b], V. Ciriolo [a,b,15], S. Di Guida [a,b,15], M.E. Dinardo [a,b], S. Fiorendi [a,b],
S. Gennai [a], A. Ghezzi [a,b], P. Govoni [a,b], M. Malberti [a,b], S. Malvezzi [a], A. Massironi [a,b], D. Menasce [a],
F. Monti, L. Moroni [a], M. Paganoni [a,b], D. Pedrini [a], S. Ragazzi [a,b], T. Tabarelli de Fatis [a,b], D. Zuolo [a,b]

[a] *INFN Sezione di Milano-Bicocca, Milano, Italy*
[b] *Università di Milano-Bicocca, Milano, Italy*

S. Buontempo [a], N. Cavallo [a,c], A. De Iorio [a,b], A. Di Crescenzo [a,b], F. Fabozzi [a,c], F. Fienga [a], G. Galati [a],
A.O.M. Iorio [a,b], W.A. Khan [a], L. Lista [a], S. Meola [a,d,15], P. Paolucci [a,15], C. Sciacca [a,b], E. Voevodina [a,b]

[a] *INFN Sezione di Napoli, Napoli, Italy*
[b] *Università di Napoli 'Federico II', Napoli, Italy*
[c] *Università della Basilicata, Potenza, Italy*
[d] *Università G. Marconi, Roma, Italy*

P. Azzi [a], N. Bacchetta [a], D. Bisello [a,b], A. Boletti [a,b], A. Bragagnolo, R. Carlin [a,b], P. Checchia [a],
M. Dall'Osso [a,b], P. De Castro Manzano [a], T. Dorigo [a], U. Dosselli [a], U. Gasparini [a,b], A. Gozzelino [a], S.Y. Hoh,
S. Lacaprara [a], P. Lujan, M. Margoni [a,b], A.T. Meneguzzo [a,b], J. Pazzini [a,b], N. Pozzobon [a,b], P. Ronchese [a,b],
R. Rossin [a,b], F. Simonetto [a,b], A. Tiko, E. Torassa [a], M. Tosi [a,b], M. Zanetti [a,b], P. Zotto [a,b], G. Zumerle [a,b]

[a] *INFN Sezione di Padova, Padova, Italy*
[b] *Università di Padova, Padova, Italy*
[c] *Università di Trento, Trento, Italy*

A. Braghieri [a], A. Magnani [a], P. Montagna [a,b], S.P. Ratti [a,b], V. Re [a], M. Ressegotti [a,b], C. Riccardi [a,b],
P. Salvini [a], I. Vai [a,b], P. Vitulo [a,b]

[a] *INFN Sezione di Pavia, Pavia, Italy*
[b] *Università di Pavia, Pavia, Italy*

M. Biasini [a,b], G.M. Bilei [a], C. Cecchi [a,b], D. Ciangottini [a,b], L. Fanò [a,b], P. Lariccia [a,b], R. Leonardi [a,b],
E. Manoni [a], G. Mantovani [a,b], V. Mariani [a,b], M. Menichelli [a], A. Rossi [a,b], A. Santocchia [a,b], D. Spiga [a]

[a] *INFN Sezione di Perugia, Perugia, Italy*
[b] *Università di Perugia, Perugia, Italy*

K. Androsov [a], P. Azzurri [a], G. Bagliesi [a], L. Bianchini [a], T. Boccali [a], L. Borrello, R. Castaldi [a], M.A. Ciocci [a,b],
R. Dell'Orso [a], G. Fedi [a], F. Fiori [a,c], L. Giannini [a,c], A. Giassi [a], M.T. Grippo [a], F. Ligabue [a,c], E. Manca [a,c],
G. Mandorli [a,c], A. Messineo [a,b], F. Palla [a], A. Rizzi [a,b], G. Rolandi [28], P. Spagnolo [a], R. Tenchini [a],
G. Tonelli [a,b], A. Venturi [a], P.G. Verdini [a]

[a] *INFN Sezione di Pisa, Pisa, Italy*
[b] *Università di Pisa, Pisa, Italy*
[c] *Scuola Normale Superiore di Pisa, Pisa, Italy*

L. Barone [a,b], F. Cavallari [a], M. Cipriani [a,b], D. Del Re [a,b], E. Di Marco [a,b], M. Diemoz [a], S. Gelli [a,b], E. Longo [a,b], B. Marzocchi [a,b], P. Meridiani [a], G. Organtini [a,b], F. Pandolfi [a], R. Paramatti [a,b], F. Preiato [a,b], S. Rahatlou [a,b], C. Rovelli [a], F. Santanastasio [a,b]

[a] *INFN Sezione di Roma, Rome, Italy*
[b] *Sapienza Università di Roma, Rome, Italy*

N. Amapane [a,b], R. Arcidiacono [a,c], S. Argiro [a,b], M. Arneodo [a,c], N. Bartosik [a], R. Bellan [a,b], C. Biino [a], A. Cappati [a,b], N. Cartiglia [a], F. Cenna [a,b], S. Cometti [a], M. Costa [a,b], R. Covarelli [a,b], N. Demaria [a], B. Kiani [a,b], C. Mariotti [a], S. Maselli [a], E. Migliore [a,b], V. Monaco [a,b], E. Monteil [a,b], M. Monteno [a], M.M. Obertino [a,b], L. Pacher [a,b], N. Pastrone [a], M. Pelliccioni [a], G.L. Pinna Angioni [a,b], A. Romero [a,b], M. Ruspa [a,c], R. Sacchi [a,b], R. Salvatico [a,b], K. Shchelina [a,b], V. Sola [a], A. Solano [a,b], D. Soldi [a,b], A. Staiano [a]

[a] *INFN Sezione di Torino, Torino, Italy*
[b] *Università di Torino, Torino, Italy*
[c] *Università del Piemonte Orientale, Novara, Italy*

S. Belforte [a], V. Candelise [a,b], M. Casarsa [a], F. Cossutti [a], A. Da Rold [a,b], G. Della Ricca [a,b], F. Vazzoler [a,b], A. Zanetti [a]

[a] *INFN Sezione di Trieste, Trieste, Italy*
[b] *Università di Trieste, Trieste, Italy*

D.H. Kim, G.N. Kim, M.S. Kim, J. Lee, S. Lee, S.W. Lee, C.S. Moon, Y.D. Oh, S.I. Pak, S. Sekmen, D.C. Son, Y.C. Yang

Kyungpook National University, Daegu, Republic of Korea

H. Kim, D.H. Moon, G. Oh

Chonnam National University, Institute for Universe and Elementary Particles, Kwangju, Republic of Korea

B. Francois, J. Goh [29], T.J. Kim

Hanyang University, Seoul, Republic of Korea

S. Cho, S. Choi, Y. Go, D. Gyun, S. Ha, B. Hong, Y. Jo, K. Lee, K.S. Lee, S. Lee, J. Lim, S.K. Park, Y. Roh

Korea University, Seoul, Republic of Korea

H.S. Kim

Sejong University, Seoul, Republic of Korea

J. Almond, J. Kim, J.S. Kim, H. Lee, K. Lee, K. Nam, S.B. Oh, B.C. Radburn-Smith, S.h. Seo, U.K. Yang, H.D. Yoo, G.B. Yu

Seoul National University, Seoul, Republic of Korea

D. Jeon, H. Kim, J.H. Kim, J.S.H. Lee, I.C. Park

University of Seoul, Seoul, Republic of Korea

Y. Choi, C. Hwang, J. Lee, I. Yu

Sungkyunkwan University, Suwon, Republic of Korea

V. Dudenas, A. Juodagalvis, J. Vaitkus

Vilnius University, Vilnius, Lithuania

I. Ahmed, Z.A. Ibrahim, M.A.B. Md Ali [30], F. Mohamad Idris [31], W.A.T. Wan Abdullah, M.N. Yusli, Z. Zolkapli

National Centre for Particle Physics, Universiti Malaya, Kuala Lumpur, Malaysia

J.F. Benitez, A. Castaneda Hernandez, J.A. Murillo Quijada

Universidad de Sonora (UNISON), Hermosillo, Mexico

H. Castilla-Valdez, E. De La Cruz-Burelo, M.C. Duran-Osuna, I. Heredia-De La Cruz [32], R. Lopez-Fernandez, J. Mejia Guisao, R.I. Rabadan-Trejo, M. Ramirez-Garcia, G. Ramirez-Sanchez, R. Reyes-Almanza, A. Sanchez-Hernandez

Centro de Investigacion y de Estudios Avanzados del IPN, Mexico City, Mexico

S. Carrillo Moreno, C. Oropeza Barrera, F. Vazquez Valencia

Universidad Iberoamericana, Mexico City, Mexico

J. Eysermans, I. Pedraza, H.A. Salazar Ibarguen, C. Uribe Estrada

Benemerita Universidad Autonoma de Puebla, Puebla, Mexico

A. Morelos Pineda

Universidad Autónoma de San Luis Potosí, San Luis Potosí, Mexico

D. Krofcheck

University of Auckland, Auckland, New Zealand

S. Bheesette, P.H. Butler

University of Canterbury, Christchurch, New Zealand

A. Ahmad, M. Ahmad, M.I. Asghar, Q. Hassan, H.R. Hoorani, A. Saddique, M.A. Shah, M. Shoaib, M. Waqas

National Centre for Physics, Quaid-I-Azam University, Islamabad, Pakistan

H. Bialkowska, M. Bluj, B. Boimska, T. Frueboes, M. Górski, M. Kazana, M. Szleper, P. Traczyk, P. Zalewski

National Centre for Nuclear Research, Swierk, Poland

K. Bunkowski, A. Byszuk [33], K. Doroba, A. Kalinowski, M. Konecki, J. Krolikowski, M. Misiura, M. Olszewski, A. Pyskir, M. Walczak

Institute of Experimental Physics, Faculty of Physics, University of Warsaw, Warsaw, Poland

M. Araujo, P. Bargassa, C. Beirão Da Cruz E Silva, A. Di Francesco, P. Faccioli, B. Galinhas, M. Gallinaro, J. Hollar, N. Leonardo, J. Seixas, G. Strong, O. Toldaiev, J. Varela

Laboratório de Instrumentação e Física Experimental de Partículas, Lisboa, Portugal

S. Afanasiev, P. Bunin, M. Gavrilenko, I. Golutvin, I. Gorbunov, A. Kamenev, V. Karjavine, A. Lanev, A. Malakhov, V. Matveev [34,35], P. Moisenz, V. Palichik, V. Perelygin, S. Shmatov, S. Shulha, N. Skatchkov, V. Smirnov, N. Voytishin, A. Zarubin

Joint Institute for Nuclear Research, Dubna, Russia

V. Golovtsov, Y. Ivanov, V. Kim [36], E. Kuznetsova [37], P. Levchenko, V. Murzin, V. Oreshkin, I. Smirnov, D. Sosnov, V. Sulimov, L. Uvarov, S. Vavilov, A. Vorobyev

Petersburg Nuclear Physics Institute, Gatchina (St. Petersburg), Russia

Yu. Andreev, A. Dermenev, S. Gninenko, N. Golubev, A. Karneyeu, M. Kirsanov, N. Krasnikov, A. Pashenkov, D. Tlisov, A. Toropin

Institute for Nuclear Research, Moscow, Russia

V. Epshteyn, V. Gavrilov, N. Lychkovskaya, V. Popov, I. Pozdnyakov, G. Safronov, A. Spiridonov, A. Stepennov, V. Stolin, M. Toms, E. Vlasov, A. Zhokin

Institute for Theoretical and Experimental Physics, Moscow, Russia

T. Aushev

Moscow Institute of Physics and Technology, Moscow, Russia

R. Chistov [38], M. Danilov [38], P. Parygin, D. Philippov, S. Polikarpov [38], E. Tarkovskii

National Research Nuclear University 'Moscow Engineering Physics Institute' (MEPhI), Moscow, Russia

V. Andreev, M. Azarkin, I. Dremin [35], M. Kirakosyan, A. Terkulov

P.N. Lebedev Physical Institute, Moscow, Russia

A. Baskakov, A. Belyaev, E. Boos, M. Dubinin [39], L. Dudko, A. Ershov, A. Gribushin, V. Klyukhin, O. Kodolova, I. Lokhtin, I. Miagkov, S. Obraztsov, S. Petrushanko, V. Savrin, A. Snigirev

Skobeltsyn Institute of Nuclear Physics, Lomonosov Moscow State University, Moscow, Russia

A. Barnyakov [40], V. Blinov [40], T. Dimova [40], L. Kardapoltsev [40], Y. Skovpen [40]

Novosibirsk State University (NSU), Novosibirsk, Russia

I. Azhgirey, I. Bayshev, S. Bitioukov, D. Elumakhov, A. Godizov, V. Kachanov, A. Kalinin, D. Konstantinov, P. Mandrik, V. Petrov, R. Ryutin, S. Slabospitskii, A. Sobol, S. Troshin, N. Tyurin, A. Uzunian, A. Volkov

Institute for High Energy Physics of National Research Centre 'Kurchatov Institute', Protvino, Russia

A. Babaev, S. Baidali, V. Okhotnikov

National Research Tomsk Polytechnic University, Tomsk, Russia

P. Adzic [41], P. Cirkovic, D. Devetak, M. Dordevic, J. Milosevic

University of Belgrade, Faculty of Physics and Vinca Institute of Nuclear Sciences, Belgrade, Serbia

J. Alcaraz Maestre, A. Álvarez Fernández, I. Bachiller, M. Barrio Luna, J.A. Brochero Cifuentes, M. Cerrada, N. Colino, B. De La Cruz, A. Delgado Peris, C. Fernandez Bedoya, J.P. Fernández Ramos, J. Flix, M.C. Fouz, O. Gonzalez Lopez, S. Goy Lopez, J.M. Hernandez, M.I. Josa, D. Moran, A. Pérez-Calero Yzquierdo, J. Puerta Pelayo, I. Redondo, L. Romero, M.S. Soares, A. Triossi

Centro de Investigaciones Energéticas Medioambientales y Tecnológicas (CIEMAT), Madrid, Spain

C. Albajar, J.F. de Trocóniz

Universidad Autónoma de Madrid, Madrid, Spain

J. Cuevas, C. Erice, J. Fernandez Menendez, S. Folgueras, I. Gonzalez Caballero, J.R. González Fernández, E. Palencia Cortezon, V. Rodríguez Bouza, S. Sanchez Cruz, P. Vischia, J.M. Vizan Garcia

Universidad de Oviedo, Oviedo, Spain

I.J. Cabrillo, A. Calderon, B. Chazin Quero, J. Duarte Campderros, M. Fernandez, P.J. Fernández Manteca, A. García Alonso, J. Garcia-Ferrero, G. Gomez, A. Lopez Virto, J. Marco, C. Martinez Rivero, P. Martinez Ruiz del Arbol, F. Matorras, J. Piedra Gomez, C. Prieels, T. Rodrigo, A. Ruiz-Jimeno, L. Scodellaro, N. Trevisani, I. Vila, R. Vilar Cortabitarte

Instituto de Física de Cantabria (IFCA), CSIC-Universidad de Cantabria, Santander, Spain

N. Wickramage

University of Ruhuna, Department of Physics, Matara, Sri Lanka

D. Abbaneo, B. Akgun, E. Auffray, G. Auzinger, P. Baillon, A.H. Ball, D. Barney, J. Bendavid, M. Bianco, A. Bocci, C. Botta, E. Brondolin, T. Camporesi, M. Cepeda, G. Cerminara, E. Chapon, Y. Chen, G. Cucciati, D. d'Enterria, A. Dabrowski, N. Daci, V. Daponte, A. David, A. De Roeck, N. Deelen, M. Dobson,

M. Dünser, N. Dupont, A. Elliott-Peisert, P. Everaerts, F. Fallavollita [42], D. Fasanella, G. Franzoni, J. Fulcher, W. Funk, D. Gigi, A. Gilbert, K. Gill, F. Glege, M. Gruchala, M. Guilbaud, D. Gulhan, J. Hegeman, C. Heidegger, V. Innocente, A. Jafari, P. Janot, O. Karacheban [18], J. Kieseler, A. Kornmayer, M. Krammer [1], C. Lange, P. Lecoq, C. Lourenço, L. Malgeri, M. Mannelli, F. Meijers, J.A. Merlin, S. Mersi, E. Meschi, P. Milenovic [43], F. Moortgat, M. Mulders, J. Ngadiuba, S. Nourbakhsh, S. Orfanelli, L. Orsini, F. Pantaleo [15], L. Pape, E. Perez, M. Peruzzi, A. Petrilli, G. Petrucciani, A. Pfeiffer, M. Pierini, F.M. Pitters, D. Rabady, A. Racz, T. Reis, M. Rovere, H. Sakulin, C. Schäfer, C. Schwick, M. Seidel, M. Selvaggi, A. Sharma, P. Silva, P. Sphicas [44], A. Stakia, J. Steggemann, D. Treille, A. Tsirou, V. Veckalns [45], M. Verzetti, W.D. Zeuner

CERN, European Organization for Nuclear Research, Geneva, Switzerland

L. Caminada [46], K. Deiters, W. Erdmann, R. Horisberger, Q. Ingram, H.C. Kaestli, D. Kotlinski, U. Langenegger, T. Rohe, S.A. Wiederkehr

Paul Scherrer Institut, Villigen, Switzerland

M. Backhaus, L. Bäni, P. Berger, N. Chernyavskaya, G. Dissertori, M. Dittmar, M. Donegà, C. Dorfer, T.A. Gómez Espinosa, C. Grab, D. Hits, T. Klijnsma, W. Lustermann, R.A. Manzoni, M. Marionneau, M.T. Meinhard, F. Micheli, P. Musella, F. Nessi-Tedaldi, J. Pata, F. Pauss, G. Perrin, L. Perrozzi, S. Pigazzini, M. Quittnat, C. Reissel, D. Ruini, D.A. Sanz Becerra, M. Schönenberger, L. Shchutska, V.R. Tavolaro, K. Theofilatos, M.L. Vesterbacka Olsson, R. Wallny, D.H. Zhu

ETH Zurich – Institute for Particle Physics and Astrophysics (IPA), Zurich, Switzerland

T.K. Aarrestad, C. Amsler [47], D. Brzhechko, M.F. Canelli, A. De Cosa, R. Del Burgo, S. Donato, C. Galloni, T. Hreus, B. Kilminster, S. Leontsinis, I. Neutelings, G. Rauco, P. Robmann, D. Salerno, K. Schweiger, C. Seitz, Y. Takahashi, A. Zucchetta

Universität Zürich, Zurich, Switzerland

T.H. Doan, R. Khurana, C.M. Kuo, W. Lin, A. Pozdnyakov, S.S. Yu

National Central University, Chung-Li, Taiwan

P. Chang, Y. Chao, K.F. Chen, P.H. Chen, W.-S. Hou, Arun Kumar, Y.F. Liu, R.-S. Lu, E. Paganis, A. Psallidas, A. Steen

National Taiwan University (NTU), Taipei, Taiwan

B. Asavapibhop, N. Srimanobhas, N. Suwonjandee

Chulalongkorn University, Faculty of Science, Department of Physics, Bangkok, Thailand

A. Bat, F. Boran, S. Damarseckin, Z.S. Demiroglu, F. Dolek, C. Dozen, I. Dumanoglu, S. Girgis, G. Gokbulut, Y. Guler, E. Gurpinar, I. Hos [48], C. Isik, E.E. Kangal [49], O. Kara, A. Kayis Topaksu, U. Kiminsu, M. Oglakci, G. Onengut, K. Ozdemir [50], S. Ozturk [51], D. Sunar Cerci [52], B. Tali [52], U.G. Tok, H. Topakli [51], S. Turkcapar, I.S. Zorbakir, C. Zorbilmez

Çukurova University, Physics Department, Science and Art Faculty, Adana, Turkey

B. Isildak [53], G. Karapinar [54], M. Yalvac, M. Zeyrek

Middle East Technical University, Physics Department, Ankara, Turkey

I.O. Atakisi, E. Gülmez, M. Kaya [55], O. Kaya [56], S. Ozkorucuklu [57], S. Tekten, E.A. Yetkin [58]

Bogazici University, Istanbul, Turkey

M.N. Agaras, A. Cakir, K. Cankocak, Y. Komurcu, S. Sen [59]

Istanbul Technical University, Istanbul, Turkey

B. Grynyov

Institute for Scintillation Materials of National Academy of Science of Ukraine, Kharkov, Ukraine

L. Levchuk

National Scientific Center, Kharkov Institute of Physics and Technology, Kharkov, Ukraine

F. Ball, J.J. Brooke, D. Burns, E. Clement, D. Cussans, O. Davignon, H. Flacher, J. Goldstein, G.P. Heath, H.F. Heath, L. Kreczko, D.M. Newbold [60], S. Paramesvaran, B. Penning, T. Sakuma, D. Smith, V.J. Smith, J. Taylor, A. Titterton

University of Bristol, Bristol, United Kingdom

K.W. Bell, A. Belyaev [61], C. Brew, R.M. Brown, D. Cieri, D.J.A. Cockerill, J.A. Coughlan, K. Harder, S. Harper, J. Linacre, E. Olaiya, D. Petyt, C.H. Shepherd-Themistocleous, A. Thea, I.R. Tomalin, T. Williams, W.J. Womersley

Rutherford Appleton Laboratory, Didcot, United Kingdom

R. Bainbridge, P. Bloch, J. Borg, S. Breeze, O. Buchmuller, A. Bundock, D. Colling, P. Dauncey, G. Davies, M. Della Negra, R. Di Maria, G. Hall, G. Iles, T. James, M. Komm, C. Laner, L. Lyons, A.-M. Magnan, S. Malik, A. Martelli, J. Nash [62], A. Nikitenko [7], V. Palladino, M. Pesaresi, D.M. Raymond, A. Richards, A. Rose, E. Scott, C. Seez, A. Shtipliyski, G. Singh, M. Stoye, T. Strebler, S. Summers, A. Tapper, K. Uchida, T. Virdee [15], N. Wardle, D. Winterbottom, J. Wright, S.C. Zenz

Imperial College, London, United Kingdom

J.E. Cole, P.R. Hobson, A. Khan, P. Kyberd, C.K. Mackay, A. Morton, I.D. Reid, L. Teodorescu, S. Zahid

Brunel University, Uxbridge, United Kingdom

K. Call, J. Dittmann, K. Hatakeyama, H. Liu, C. Madrid, B. McMaster, N. Pastika, C. Smith

Baylor University, Waco, USA

R. Bartek, A. Dominguez

Catholic University of America, Washington, DC, USA

A. Buccilli, S.I. Cooper, C. Henderson, P. Rumerio, C. West

The University of Alabama, Tuscaloosa, USA

D. Arcaro, T. Bose, D. Gastler, D. Pinna, D. Rankin, C. Richardson, J. Rohlf, L. Sulak, D. Zou

Boston University, Boston, USA

G. Benelli, X. Coubez, D. Cutts, M. Hadley, J. Hakala, U. Heintz, J.M. Hogan [63], K.H.M. Kwok, E. Laird, G. Landsberg, J. Lee, Z. Mao, M. Narain, S. Sagir [64], R. Syarif, E. Usai, D. Yu

Brown University, Providence, USA

R. Band, C. Brainerd, R. Breedon, D. Burns, M. Calderon De La Barca Sanchez, M. Chertok, J. Conway, R. Conway, P.T. Cox, R. Erbacher, C. Flores, G. Funk, W. Ko, O. Kukral, R. Lander, M. Mulhearn, D. Pellett, J. Pilot, S. Shalhout, M. Shi, D. Stolp, D. Taylor, K. Tos, M. Tripathi, Z. Wang, F. Zhang

University of California, Davis, Davis, USA

M. Bachtis, C. Bravo, R. Cousins, A. Dasgupta, A. Florent, J. Hauser, M. Ignatenko, N. Mccoll, S. Regnard, D. Saltzberg, C. Schnaible, V. Valuev

University of California, Los Angeles, USA

E. Bouvier, K. Burt, R. Clare, J.W. Gary, S.M.A. Ghiasi Shirazi, G. Hanson, G. Karapostoli, E. Kennedy, F. Lacroix, O.R. Long, M. Olmedo Negrete, M.I. Paneva, W. Si, L. Wang, H. Wei, S. Wimpenny, B.R. Yates

University of California, Riverside, Riverside, USA

J.G. Branson, P. Chang, S. Cittolin, M. Derdzinski, R. Gerosa, D. Gilbert, B. Hashemi, A. Holzner, D. Klein, G. Kole, V. Krutelyov, J. Letts, M. Masciovecchio, D. Olivito, S. Padhi, M. Pieri, M. Sani, V. Sharma, S. Simon, M. Tadel, A. Vartak, S. Wasserbaech [65], J. Wood, F. Würthwein, A. Yagil, G. Zevi Della Porta

University of California, San Diego, La Jolla, USA

N. Amin, R. Bhandari, C. Campagnari, M. Citron, V. Dutta, M. Franco Sevilla, L. Gouskos, R. Heller, J. Incandela, A. Ovcharova, H. Qu, J. Richman, D. Stuart, I. Suarez, S. Wang, J. Yoo

University of California, Santa Barbara – Department of Physics, Santa Barbara, USA

D. Anderson, A. Bornheim, J.M. Lawhorn, N. Lu, H.B. Newman, T.Q. Nguyen, M. Spiropulu, J.R. Vlimant, R. Wilkinson, S. Xie, Z. Zhang, R.Y. Zhu

California Institute of Technology, Pasadena, USA

M.B. Andrews, T. Ferguson, T. Mudholkar, M. Paulini, M. Sun, I. Vorobiev, M. Weinberg

Carnegie Mellon University, Pittsburgh, USA

J.P. Cumalat, W.T. Ford, F. Jensen, A. Johnson, E. MacDonald, T. Mulholland, R. Patel, A. Perloff, K. Stenson, K.A. Ulmer, S.R. Wagner

University of Colorado Boulder, Boulder, USA

J. Alexander, J. Chaves, Y. Cheng, J. Chu, A. Datta, K. Mcdermott, N. Mirman, J.R. Patterson, D. Quach, A. Rinkevicius, A. Ryd, L. Skinnari, L. Soffi, S.M. Tan, Z. Tao, J. Thom, J. Tucker, P. Wittich, M. Zientek

Cornell University, Ithaca, USA

S. Abdullin, M. Albrow, M. Alyari, G. Apollinari, A. Apresyan, A. Apyan, S. Banerjee, L.A.T. Bauerdick, A. Beretvas, J. Berryhill, P.C. Bhat, K. Burkett, J.N. Butler, A. Canepa, G.B. Cerati, H.W.K. Cheung, F. Chlebana, M. Cremonesi, J. Duarte, V.D. Elvira, J. Freeman, Z. Gecse, E. Gottschalk, L. Gray, D. Green, S. Grünendahl, O. Gutsche, J. Hanlon, R.M. Harris, S. Hasegawa, J. Hirschauer, Z. Hu, B. Jayatilaka, S. Jindariani, M. Johnson, U. Joshi, B. Klima, M.J. Kortelainen, B. Kreis, S. Lammel, D. Lincoln, R. Lipton, M. Liu, T. Liu, J. Lykken, K. Maeshima, J.M. Marraffino, D. Mason, P. McBride, P. Merkel, S. Mrenna, S. Nahn, V. O'Dell, K. Pedro, C. Pena, O. Prokofyev, G. Rakness, L. Ristori, A. Savoy-Navarro [66], B. Schneider, E. Sexton-Kennedy, A. Soha, W.J. Spalding, L. Spiegel, S. Stoynev, J. Strait, N. Strobbe, L. Taylor, S. Tkaczyk, N.V. Tran, L. Uplegger, E.W. Vaandering, C. Vernieri, M. Verzocchi, R. Vidal, M. Wang, H.A. Weber, A. Whitbeck

Fermi National Accelerator Laboratory, Batavia, USA

D. Acosta, P. Avery, P. Bortignon, D. Bourilkov, A. Brinkerhoff, L. Cadamuro, A. Carnes, D. Curry, R.D. Field, S.V. Gleyzer, B.M. Joshi, J. Konigsberg, A. Korytov, K.H. Lo, P. Ma, K. Matchev, H. Mei, G. Mitselmakher, D. Rosenzweig, K. Shi, D. Sperka, J. Wang, S. Wang, X. Zuo

University of Florida, Gainesville, USA

Y.R. Joshi, S. Linn

Florida International University, Miami, USA

A. Ackert, T. Adams, A. Askew, S. Hagopian, V. Hagopian, K.F. Johnson, T. Kolberg, G. Martinez, T. Perry, H. Prosper, A. Saha, C. Schiber, R. Yohay

Florida State University, Tallahassee, USA

M.M. Baarmand, V. Bhopatkar, S. Colafranceschi, M. Hohlmann, D. Noonan, M. Rahmani, T. Roy, F. Yumiceva

Florida Institute of Technology, Melbourne, USA

M.R. Adams, L. Apanasevich, D. Berry, R.R. Betts, R. Cavanaugh, X. Chen, S. Dittmer, O. Evdokimov, C.E. Gerber, D.A. Hangal, D.J. Hofman, K. Jung, J. Kamin, C. Mills, I.D. Sandoval Gonzalez, M.B. Tonjes, H. Trauger, N. Varelas, H. Wang, X. Wang, Z. Wu, J. Zhang

University of Illinois at Chicago (UIC), Chicago, USA

M. Alhusseini, B. Bilki [67], W. Clarida, K. Dilsiz [68], S. Durgut, R.P. Gandrajula, M. Haytmyradov, V. Khristenko, J.-P. Merlo, A. Mestvirishvili, A. Moeller, J. Nachtman, H. Ogul [69], Y. Onel, F. Ozok [70], A. Penzo, C. Snyder, E. Tiras, J. Wetzel

The University of Iowa, Iowa City, USA

B. Blumenfeld, A. Cocoros, N. Eminizer, D. Fehling, L. Feng, A.V. Gritsan, W.T. Hung, P. Maksimovic, J. Roskes, U. Sarica, M. Swartz, M. Xiao, C. You

Johns Hopkins University, Baltimore, USA

A. Al-bataineh, P. Baringer, A. Bean, S. Boren, J. Bowen, A. Bylinkin, J. Castle, S. Khalil, A. Kropivnitskaya, D. Majumder, W. Mcbrayer, M. Murray, C. Rogan, S. Sanders, E. Schmitz, J.D. Tapia Takaki, Q. Wang

The University of Kansas, Lawrence, USA

S. Duric, A. Ivanov, K. Kaadze, D. Kim, Y. Maravin, D.R. Mendis, T. Mitchell, A. Modak, A. Mohammadi, L.K. Saini

Kansas State University, Manhattan, USA

F. Rebassoo, D. Wright

Lawrence Livermore National Laboratory, Livermore, USA

A. Baden, O. Baron, A. Belloni, S.C. Eno, Y. Feng, C. Ferraioli, N.J. Hadley, S. Jabeen, G.Y. Jeng, R.G. Kellogg, J. Kunkle, A.C. Mignerey, S. Nabili, F. Ricci-Tam, Y.H. Shin, A. Skuja, S.C. Tonwar, K. Wong

University of Maryland, College Park, USA

D. Abercrombie, B. Allen, V. Azzolini, A. Baty, G. Bauer, R. Bi, S. Brandt, W. Busza, I.A. Cali, M. D'Alfonso, Z. Demiragli, G. Gomez Ceballos, M. Goncharov, P. Harris, D. Hsu, M. Hu, Y. Iiyama, G.M. Innocenti, M. Klute, D. Kovalskyi, Y.-J. Lee, P.D. Luckey, B. Maier, A.C. Marini, C. Mcginn, C. Mironov, S. Narayanan, X. Niu, C. Paus, C. Roland, G. Roland, Z. Shi, G.S.F. Stephans, K. Sumorok, K. Tatar, D. Velicanu, J. Wang, T.W. Wang, B. Wyslouch

Massachusetts Institute of Technology, Cambridge, USA

A.C. Benvenuti [†], R.M. Chatterjee, A. Evans, P. Hansen, J. Hiltbrand, Sh. Jain, S. Kalafut, M. Krohn, Y. Kubota, Z. Lesko, J. Mans, N. Ruckstuhl, R. Rusack, M.A. Wadud

University of Minnesota, Minneapolis, USA

J.G. Acosta, S. Oliveros

University of Mississippi, Oxford, USA

E. Avdeeva, K. Bloom, D.R. Claes, C. Fangmeier, F. Golf, R. Gonzalez Suarez, R. Kamalieddin, I. Kravchenko, J. Monroy, J.E. Siado, G.R. Snow, B. Stieger

University of Nebraska-Lincoln, Lincoln, USA

A. Godshalk, C. Harrington, I. Iashvili, A. Kharchilava, C. Mclean, D. Nguyen, A. Parker, S. Rappoccio, B. Roozbahani

State University of New York at Buffalo, Buffalo, USA

G. Alverson, E. Barberis, C. Freer, Y. Haddad, A. Hortiangtham, D.M. Morse, T. Orimoto, R. Teixeira De Lima, T. Wamorkar, B. Wang, A. Wisecarver, D. Wood

Northeastern University, Boston, USA

S. Bhattacharya, J. Bueghly, O. Charaf, K.A. Hahn, N. Mucia, N. Odell, M.H. Schmitt, K. Sung, M. Trovato, M. Velasco

Northwestern University, Evanston, USA

R. Bucci, N. Dev, M. Hildreth, K. Hurtado Anampa, C. Jessop, D.J. Karmgard, N. Kellams, K. Lannon, W. Li, N. Loukas, N. Marinelli, F. Meng, C. Mueller, Y. Musienko [34], M. Planer, A. Reinsvold, R. Ruchti, P. Siddireddy, G. Smith, S. Taroni, M. Wayne, A. Wightman, M. Wolf, A. Woodard

University of Notre Dame, Notre Dame, USA

J. Alimena, L. Antonelli, B. Bylsma, L.S. Durkin, S. Flowers, B. Francis, C. Hill, W. Ji, T.Y. Ling, W. Luo, B.L. Winer

The Ohio State University, Columbus, USA

S. Cooperstein, P. Elmer, J. Hardenbrook, S. Higginbotham, A. Kalogeropoulos, D. Lange, M.T. Lucchini, J. Luo, D. Marlow, K. Mei, I. Ojalvo, J. Olsen, C. Palmer, P. Piroué, J. Salfeld-Nebgen, D. Stickland, C. Tully, Z. Wang

Princeton University, Princeton, USA

S. Malik, S. Norberg

University of Puerto Rico, Mayaguez, USA

A. Barker, V.E. Barnes, S. Das, L. Gutay, M. Jones, A.W. Jung, A. Khatiwada, B. Mahakud, D.H. Miller, N. Neumeister, C.C. Peng, S. Piperov, H. Qiu, J.F. Schulte, J. Sun, F. Wang, R. Xiao, W. Xie

Purdue University, West Lafayette, USA

T. Cheng, J. Dolen, N. Parashar

Purdue University Northwest, Hammond, USA

Z. Chen, K.M. Ecklund, S. Freed, F.J.M. Geurts, M. Kilpatrick, W. Li, B.P. Padley, R. Redjimi, J. Roberts, J. Rorie, W. Shi, Z. Tu, A. Zhang

Rice University, Houston, USA

A. Bodek, P. de Barbaro, R. Demina, Y.t. Duh, J.L. Dulemba, C. Fallon, T. Ferbel, M. Galanti, A. Garcia-Bellido, J. Han, O. Hindrichs, A. Khukhunaishvili, E. Ranken, P. Tan, R. Taus

University of Rochester, Rochester, USA

A. Agapitos, J.P. Chou, Y. Gershtein, E. Halkiadakis, A. Hart, M. Heindl, E. Hughes, S. Kaplan, R. Kunnawalkam Elayavalli, S. Kyriacou, A. Lath, R. Montalvo, K. Nash, M. Osherson, H. Saka, S. Salur, S. Schnetzer, D. Sheffield, S. Somalwar, R. Stone, S. Thomas, P. Thomassen, M. Walker

Rutgers, The State University of New Jersey, Piscataway, USA

A.G. Delannoy, J. Heideman, G. Riley, S. Spanier

University of Tennessee, Knoxville, USA

O. Bouhali [71], A. Celik, M. Dalchenko, M. De Mattia, A. Delgado, S. Dildick, R. Eusebi, J. Gilmore, T. Huang, T. Kamon [72], S. Luo, R. Mueller, D. Overton, L. Perniè, D. Rathjens, A. Safonov

Texas A&M University, College Station, USA

N. Akchurin, J. Damgov, F. De Guio, P.R. Dudero, S. Kunori, K. Lamichhane, S.W. Lee, T. Mengke, S. Muthumuni, T. Peltola, S. Undleeb, I. Volobouev, Z. Wang

Texas Tech University, Lubbock, USA

S. Greene, A. Gurrola, R. Janjam, W. Johns, C. Maguire, A. Melo, H. Ni, K. Padeken, J.D. Ruiz Alvarez, P. Sheldon, S. Tuo, J. Velkovska, M. Verweij, Q. Xu

Vanderbilt University, Nashville, USA

M.W. Arenton, P. Barria, B. Cox, R. Hirosky, M. Joyce, A. Ledovskoy, H. Li, C. Neu, T. Sinthuprasith, Y. Wang, E. Wolfe, F. Xia

University of Virginia, Charlottesville, USA

R. Harr, P.E. Karchin, N. Poudyal, J. Sturdy, P. Thapa, S. Zaleski

Wayne State University, Detroit, USA

M. Brodski, J. Buchanan, C. Caillol, D. Carlsmith, S. Dasu, I. De Bruyn, L. Dodd, B. Gomber, M. Grothe, M. Herndon, A. Hervé, U. Hussain, P. Klabbers, A. Lanaro, K. Long, R. Loveless, T. Ruggles, A. Savin, V. Sharma, N. Smith, W.H. Smith, N. Woods

University of Wisconsin – Madison, Madison, WI, USA

[†] Deceased.
[1] Also at Vienna University of Technology, Vienna, Austria.
[2] Also at IRFU, CEA, Université Paris-Saclay, Gif-sur-Yvette, France.
[3] Also at Universidade Estadual de Campinas, Campinas, Brazil.
[4] Also at Federal University of Rio Grande do Sul, Porto Alegre, Brazil.
[5] Also at Université Libre de Bruxelles, Bruxelles, Belgium.
[6] Also at University of Chinese Academy of Sciences, Beijing, China.
[7] Also at Institute for Theoretical and Experimental Physics, Moscow, Russia.
[8] Also at Joint Institute for Nuclear Research, Dubna, Russia.
[9] Also at Cairo University, Cairo, Egypt.
[10] Also at Helwan University, Cairo, Egypt.
[11] Now at Zewail City of Science and Technology, Zewail, Egypt.
[12] Also at Department of Physics, King Abdulaziz University, Jeddah, Saudi Arabia.
[13] Also at Université de Haute Alsace, Mulhouse, France.
[14] Also at Skobeltsyn Institute of Nuclear Physics, Lomonosov Moscow State University, Moscow, Russia.
[15] Also at CERN, European Organization for Nuclear Research, Geneva, Switzerland.
[16] Also at RWTH Aachen University, III. Physikalisches Institut A, Aachen, Germany.
[17] Also at University of Hamburg, Hamburg, Germany.
[18] Also at Brandenburg University of Technology, Cottbus, Germany.
[19] Also at Institute of Physics, University of Debrecen, Debrecen, Hungary.
[20] Also at Institute of Nuclear Research ATOMKI, Debrecen, Hungary.
[21] Also at Indian Institute of Technology Bhubaneswar, Bhubaneswar, India.
[22] Also at Institute of Physics, Bhubaneswar, India.
[23] Also at Shoolini University, Solan, India.
[24] Also at University of Visva-Bharati, Santiniketan, India.
[25] Also at Isfahan University of Technology, Isfahan, Iran.
[26] Also at Plasma Physics Research Center, Science and Research Branch, Islamic Azad University, Tehran, Iran.
[27] Also at Università degli Studi di Siena, Siena, Italy.
[28] Also at Scuola Normale e Sezione dell'INFN, Pisa, Italy.
[29] Also at Kyunghee University, Seoul, Republic of Korea.
[30] Also at International Islamic University of Malaysia, Kuala Lumpur, Malaysia.
[31] Also at Malaysian Nuclear Agency, MOSTI, Kajang, Malaysia.
[32] Also at Consejo Nacional de Ciencia y Tecnología, Mexico City, Mexico.
[33] Also at Warsaw University of Technology, Institute of Electronic Systems, Warsaw, Poland.
[34] Also at Institute for Nuclear Research, Moscow, Russia.
[35] Now at National Research Nuclear University 'Moscow Engineering Physics Institute' (MEPhI), Moscow, Russia.
[36] Also at St. Petersburg State Polytechnical University, St. Petersburg, Russia.

[37] Also at University of Florida, Gainesville, USA.

[38] Also at P.N. Lebedev Physical Institute, Moscow, Russia.

[39] Also at California Institute of Technology, Pasadena, USA.

[40] Also at Budker Institute of Nuclear Physics, Novosibirsk, Russia.

[41] Also at Faculty of Physics, University of Belgrade, Belgrade, Serbia.

[42] Also at INFN Sezione di Pavia ^{a}, Università di Pavia ^{b}, Pavia, Italy.

[43] Also at University of Belgrade, Faculty of Physics and Vinca Institute of Nuclear Sciences, Belgrade, Serbia.

[44] Also at National and Kapodistrian University of Athens, Athens, Greece.

[45] Also at Riga Technical University, Riga, Latvia.

[46] Also at Universität Zürich, Zurich, Switzerland.

[47] Also at Stefan Meyer Institute for Subatomic Physics (SMI), Vienna, Austria.

[48] Also at Istanbul Aydin University, Istanbul, Turkey.

[49] Also at Mersin University, Mersin, Turkey.

[50] Also at Piri Reis University, Istanbul, Turkey.

[51] Also at Gaziosmanpasa University, Tokat, Turkey.

[52] Also at Adiyaman University, Adiyaman, Turkey.

[53] Also at Ozyegin University, Istanbul, Turkey.

[54] Also at Izmir Institute of Technology, Izmir, Turkey.

[55] Also at Marmara University, Istanbul, Turkey.

[56] Also at Kafkas University, Kars, Turkey.

[57] Also at Istanbul University, Faculty of Science, Istanbul, Turkey.

[58] Also at Istanbul Bilgi University, Istanbul, Turkey.

[59] Also at Hacettepe University, Ankara, Turkey.

[60] Also at Rutherford Appleton Laboratory, Didcot, United Kingdom.

[61] Also at School of Physics and Astronomy, University of Southampton, Southampton, United Kingdom.

[62] Also at Monash University, Faculty of Science, Clayton, Australia.

[63] Also at Bethel University, St. Paul, USA.

[64] Also at Karamanoğlu Mehmetbey University, Karaman, Turkey.

[65] Also at Utah Valley University, Orem, USA.

[66] Also at Purdue University, West Lafayette, USA.

[67] Also at Beykent University, Istanbul, Turkey.

[68] Also at Bingol University, Bingol, Turkey.

[69] Also at Sinop University, Sinop, Turkey.

[70] Also at Mimar Sinan University, Istanbul, Istanbul, Turkey.

[71] Also at Texas A&M University at Qatar, Doha, Qatar.

[72] Also at Kyungpook National University, Daegu, Republic of Korea.